Zoological Journal of the Linnean Society, 2025, **204**(**4**), zlaf092
https://doi.org/10.1093/zoolinnean/zlaf092

OXFORD

Original Article

A new Maastrichtian hyposaurine dyrosaurid (Crocodylomorpha) from Namibe province, Angola

Arthur Maréchal[1,*], Filippo Maria Rotatori[1], Marco Merella[2], Eduardo Puértolas-Pascual[3], Cristina Sequero[1,4], Ricardo Pereira[1], Pedro Nsungani[5], Octávio Mateus[1]

[1]GeoBioTec, Departamento de Ciências da Terra, FCT, Universidade Nova de Lisboa, Caparica 2829-516, Portugal
[2]Museo di Storia Naturale, Università di Pisa, Calci 56011, Italy
[3]Departamento de Ciencias de la Tierra, Facultad de Ciencias, Aragosaurus-IUCA Reconstrucciones Palaeoambientales, Universidad de Zaragoza, Zaragoza 50009, Spain
[4]Departamento de Geodinámica, Estratigrafía y Palaeontología, Universidad Complutense de Madrid, Madrid 28040, Spain
[5]Departamento de Geologia, Faculdade de Ciências, Universidade Agostinho Neto, Luanda 374J + R8F, Angola

[*]Corresponding author. GeoBioTec, Departamento de Ciências da Terra, FCT, Universidade Nova de Lisboa, Caparica 2829-516, Portugal.
E-mail: marechal.arthur.pro@gmail.com

ABSTRACT

Dyrosauridae are one of the few clades of large marine vertebrates that survived the Cretaceous/Palaeogene (K–Pg) extinction event. The early diversification of this clade, dated to the Cretaceous, is still poorly understood. We describe a new specimen of Dyrosauridae from the Late Cretaceous of Bentiaba, Angola, represented by a posterior portion of the skull, a left ectopterygoid fragment, and a tooth. Comparative morphological analysis reveals a unique combination of characters distinguishing it from known dyrosaurid taxa but due to the fragmentary nature of the specimen and the absence of key diagnostic features, we assign it to Hyposaurinae indet.. Phylogenetic relationships were tested through maximum parsimony and Bayesian inference, using the SFBD model with time-binning criteria for the K–Pg boundary. Both of our phylogenetic analyses recover this new specimen as Hyposaurinae, which is consistent with our comparative study. Evolutionary rates accelerated during the latest stages of the Cretaceous, although the fossil bias prevents the ability to appreciate their impact on cladogenetic events. We estimated diversification, fossilization, and extinction rates, and we did not find evidence of radiation after the K–Pg in this clade. Biogeographically, this discovery supports hypotheses of longirostrine crocodyliform dispersal in Africa leading to hyposaurine diversification during the Maastrichtian.

Keywords: Africa, Bayesian analysis, Cretaceous, Gondwana, Palaeobiogeography

INTRODUCTION

The clade Crocodylomorpha is well-known for its morphological and ecological diversity throughout history, particularly during the Mesozoic (e.g. Ortega *et al.* 2000, Pol and Gasparini 2007, Young and Andrade 2009, Hastings *et al.* 2015). Over time, various crocodylomorph lineages have developed adaptations for marine or estuarine habitats, including thalattosuchians, pholidosaurids, dyrosaurids, and some longirostrine crocodylians, such as gavialoids and tomistomines (Rasmussen *et al.* 2011, Martin *et al.* 2014, Wilberg *et al.* 2019). Dyrosauridae, first erected by de Stefano in 1903, are an extinct neosuchian clade known for their extensive temporal and geographical distribution, as well as their notable evolutionary success. In de Stefano's original description (1903: 65), he stated: 'Alla nuova famiglia io darei il nome di Dyrosauridae, dall'unico rappresentante, il Dyrosaurus Pomel, che si conosce finora', which translates to: 'I would give the name Dyrosauridae to the new family, based on the only representative known so far, *Dyrosaurus* Pomel'. Subsequently, Nopcsa (1928) reclassified Dyrosauridae as the subfamily Dyrosaurinae. However, Kuhn (1966) later synonymized it with Congosauridae. The Dyrosauridae clade was later recognized by several authors and supported by phylogenetic analyses (e.g. Buffetaut 1976, 1978b, 1980, 1982, Benton and Clark 1988, Hastings *et al.* 2015, Young *et al.* 2016, Souza *et al.* 2019, Jouve and Jalil 2020). Subsequently,

Received 8 January 2025; revised 6 June 2025; accepted 12 June 2025

Jouve *et al.* proposed an emended diagnosis of the taxon in 2006. Currently, Dyrosauridae are grouped with Pholidosauridae within the clade Tethysuchia Buffetaut 1982. Recent phylogenetic analyses have supported the Dyrosauridae + Pholidosauridae grouping, reaffirming the use of Tethysuchia to represent this clade (Andrade *et al.* 2011, Fortier *et al.* 2011, Wilberg 2015, Young *et al.* 2014).

The Dyrosauroidea clade includes the non-marine early taxa *Vectisuchus* (Barremian, England) and *Elosuchus* spp. (Albian–Cenomanian, northern Africa), and the clade Dyrosauridae (Jouve *et al.* 2021). Dyrosauridae are known from the Late Cretaceous to the Eocene from South and North America, Africa, Brazil, South Asia, and possibly the Cenomanian of Europe (Jouve and Jalil 2020, and references therein). The oldest known Dyrosauridae fossils have been identified in the Campanian deposits of Kenya (Sertich *et al.* 2006) and Egypt (Saber *et al.* 2025), as well as in the Campanian–Maastrichtian deposits of Sudan (Salih *et al.* 2016, 2022). The most recent dyrosaurid record dates to the Eocene, including *Tilemsisuchus lavocati* Buffetaut, 1980 from the Lutetian of Mali, as well as two indeterminate Dyrosauridae: one from the Bartonian of India (Buffetaut 1978a) and another from the Priabonian of the USA (Ehret and Hastings 2013). Regarding the African record, material reported from Afro-Arabia includes discoveries from Algeria (Jouve 2005), Angola (Dollo 1914, Swinton 1950, Jouve and Schwarz 2004), Egypt (Churcher and Russell 1992, Lamanna *et al.* 2004, Saber *et al.* 2025), Ethiopia (Buffetaut 1982), Kenya (Sertich *et al.* 2006), Libya (Arambourg and Magnier 1961), Mali (Buffetaut 1980, Brochu *et al.* 2002, Hill *et al.* 2008), Morocco (Jouve *et al.* 2005a, b, 2006, 2008, Jouve 2005), Niger (Buffetaut 1979b, Young *et al.* 2016), Nigeria (Swinton 1930, Halstead 1975, Buffetaut 1979a, b, 1980, Jouve 2007), Togo (Amoudji *et al.* 2021), Tunisia (Thévenin 1911, Arambourg 1952, Bergounioux 1955, 1956, Buffetaut 1978b, Moody and Buffetaut 1981, Jouve 2005), Saudi Arabia (Langston 1995), Senegal (Tessier 1952, Martin *et al.* 2019), and Sudan (Buffetaut *et al.* 1990, Salih *et al.* 2016, 2022). Dyrosaurids, as a group, are typically associated with coastal and estuarine deposits, reflecting their predominantly aquatic lifestyle, either in marine or freshwater environments (Schwarz-Wings *et al.* 2009, Hastings *et al.* 2011, Wilberg *et al.* 2019). These reptiles were known for their agility in the water (Schwarz-Wings *et al.* 2009), although the possibility of a semi-aquatic lifestyle has been suggested by Andrade and de Sayão (2014). Late dyrosaurids resembled gavialoids in appearance, featuring a long, slender snout with numerous thin teeth adapted to a piscivorous diet (e.g. von Koken 1887, Barbosa *et al.* 2008). In contrast, the early dyrosaurids had a shorter rostrum with fewer and more robust teeth (Hastings *et al.* 2010, 2015, Jouve *et al.* 2005a, Young *et al.* 2016).

Advances in our understanding of the phylogenetic relationships of dyrosaurids over recent decades have significantly improved our understanding of the evolution of dyrosaurids. Evidence indicates that they probably originated from North Africa as a result of the migration of longirostrine crocodyliforms during the Late Cretaceous, as proposed by Jouve *et al.* (2005b). Subsequently, they dispersed during the Campanian and Maastrichtian to East Africa, and North and South America (Jouve *et al.* 2021). Dyrosaurids survived the Cretaceous–Palaeogene mass extinction event, although they were slightly affected by the collapse of ecosystems (Brochu 2003, Bronzati *et al.* 2015, Chiarenza *et al.* 2020, Jouve 2021). During the Palaeocene they are thought to have undergone a diversification phase, capitalizing on newly available ecological niches that had been previously occupied by marine predators, like mosasaurs and plesiosaurs (Jouve *et al.* 2008). Jouve (2021) and Jouve *et al.* (2021) suggest that dyrosaurids migrated along the coastlines of both Africa and the Americas concurrent with their diversification.

The Namibe region (South Angola) presents a rich fossil record of Upper Cretaceous–Lower Cenozoic tetrapods, encompassing dinosaurs, mosasaurs, plesiosaurs, pterosaurs, and turtles dating from the Santonian to the Palaeogene (Mateus *et al.* 2019). However, the fossil record of crocodylomorphs in Angola has been comparatively scarce, limited to *Congosaurus bequaerti* Dollo, 1914 from the Palaeogene deposits in the nearby Cabinda region (Dollo 1914, Jouve and Schwarz 2004). Here, we describe a new dyrosaurid specimen from Bentiaba, a locality in the Namibe Province (Angola), and provide phylogenetic analysis using parsimonious and Bayesian inference approaches. This new discovery expands our understanding of the geographical distribution of dyrosaurids and their dispersal to the southern hemisphere during the Maastrichtian.

The following institutional abbreviations were used in this research publication: CNRST-SUNY, Centre National pour la Recherche Scientifique et Technologique du Mali-Stony Brook University, Mali and USA; DG-CTG-UFPE, Departamento de Geologia, Centro de Tecnologia e Geociências, Universidade Federal de Pernambuco, Brazil; FCT-UNL, Faculdade de Ciências e Tecnologia, Universidade Nova de Lisboa, Caparica, Portugal; MGUAN, Museu de Geologia da Universidade Agostinho Neto, Luanda, Angola; MNHN, Muséum National d'Histoire Naturelle, Paris, France; MUVP, Mansoura University Vertebrate Palaeontology Center, Mansoura University, Egypt; NJSM, New Jersey State Museum, Trenton, NJ, USA; YPM, Yale Peabody Museum, New Haven, CT, USA.

MATERIALS AND METHODS

Geological and geographic context

The material described in this study was discovered by Octávio Mateus during fieldwork of the PalaeoAngola project in 2017. Subsequently, the specimen was curated and prepared by Marco Merella at the Museu da Lourinhã, and the NOVA University Lisbon (Portugal), which currently houses the fossil. The specimen has been accessioned to the collections of the Museu de Geologia da Universidade Agostinho Neto (Luanda) and will be returned to Angola, after completing this analysis, thus abiding by the ethical procedures of Geoheritage ownership of fossil specimens.

The specimen (MGUAN-PA548) was collected from the sandstones of a vertical cliff face at Cemitério de Bentiaba, at Bentiaba (Namibe Basin, Namibe Province, south-western Angola) (Fig. 1A, B). The deposits in which the specimen was found correspond to the Mocuio Formation, a more than 30-m thick, massive, fine-grained sandstone succession with alternating carbonate-cemented sandstone layers (Strganac *et al.* 2014, 2015a, b) (Fig. 1C), where abundant vertebrates have been recovered, including mosasaurs, turtles, and plesiosaurs (Polcyn *et al.* 2010, Araújo *et al.* 2015, Mateus *et al.* 2019, Marx *et al.* 2021,

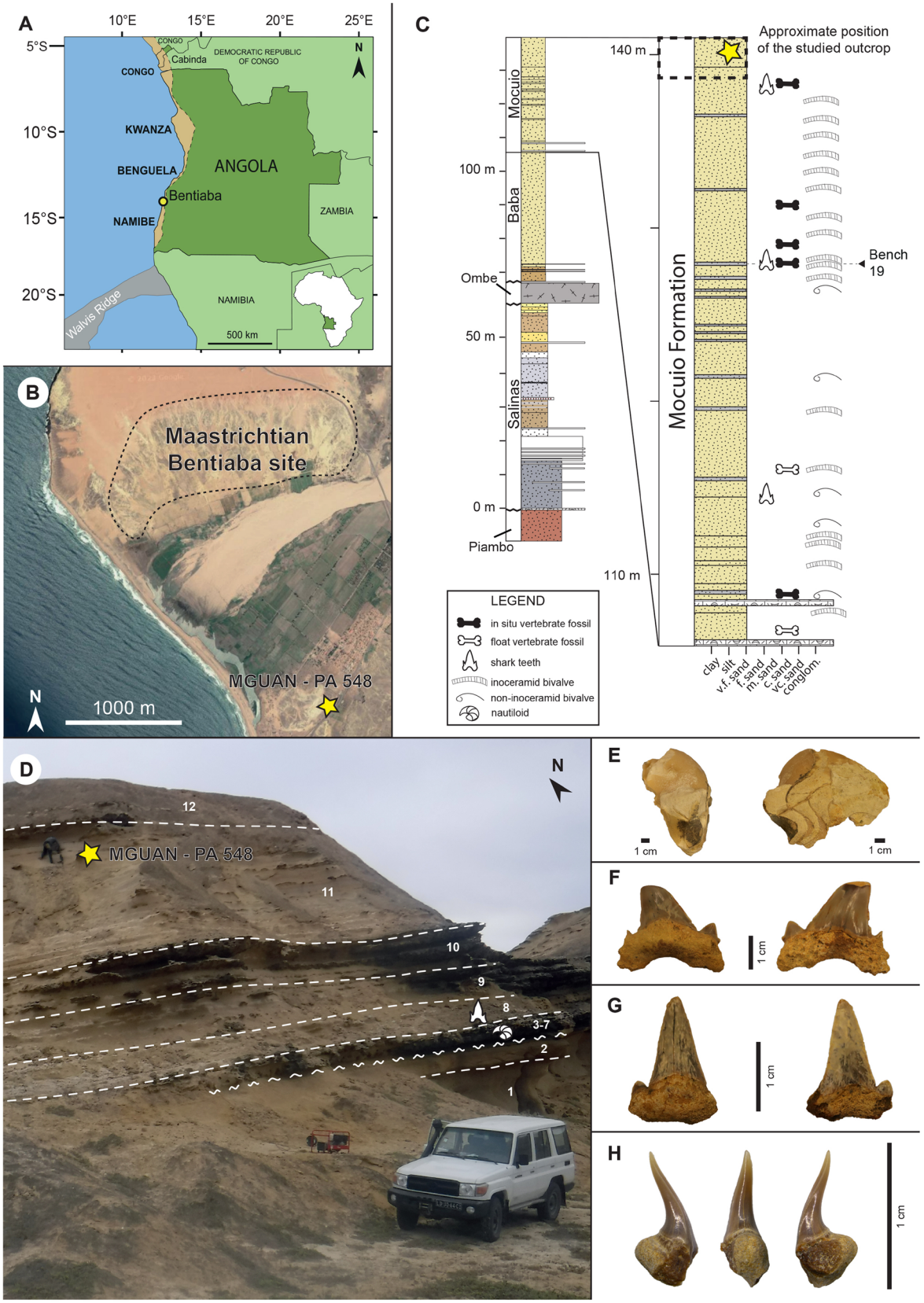

Figure 1. Location of MGUAN-PA548. A, location map of Bentiaba (modified from: Strganac *et al.* 2014; Fernandes *et al.* 2022). B, aerial view of Bentiaba area (modified from Google Earth Pro—23/01/2023; © 2023 Airbus, TerraMetrics, Data SIO, NOAA, U.S. Navy, NGA, GEBCO). C, stratigraphic section of the Bentiaba locality (modified from: Fernandes *et al.* 2022). D, outcrop photography with car as scale, with numbers indicating bedding sequence. (photo by Octávio Mateus—12/07/2019). E. *Hercoglossa* sp. fragment—MGUAN-PA 716 in apertural and side views. F, shark teeth fragments: Cretalamna maroccana—MGUAN-PA 716 in lingual and labial views. G, *Carcharias heathi*—MGUAN-PA 718 in lingual and labial views. H, *Chlamydoselachus gracilis*—MGUAN-PA 717 in lingual and profile views.

Fernandes *et al.* 2022). This succession records a narrow shallow-marine siliciclastic platform deposited at 24°S palaeolatitude (Strganac *et al.* 2015a). Water temperatures were reconstructed at *c.* 18°C based on $\delta^{18}O$ data from bivalve shells (Strganac *et al.* 2015a: 140–2). Previous geochronological, biostratigraphic, and chemostratigraphic analyses performed in a nearby succession at Bentiaba, encompassing the Mocuio Fm. (combined $\delta^{13}C$ chemostratigraphy and magnetostratigraphy), and the underlying Ombe ($^{40}Ar/^{39}Ar$ radiometric age in a basalt horizon) and Baba Fm. (using ammonite distribution) indicate a Maastrichtian age for these deposits (Cooper 1976, Strganac *et al.* 2014, 2015b).

The outcrop reveals a massive, yellow, fine-grained sandstone interval with local cross-lamination and bioturbation at the base (Fig. 1D), which transitions upwards to alternating, fine-grained sandstones and thinner carbonate-cemented sandstone layers rich in invertebrate fauna [e.g. gastropods, bivalves, and nautiloids (*Hercoglossa* sp.) (Fig. 1E)]. This section is separated from the underlying massive, fine-grained sandstone bed interval by an erosive surface, which in turn overlies a 1-cm thick glauconite-rich level. The specimen was found at the top of this outcrop, in a sandstone bed around 10 m above the erosive surface (Layer 5 in Fig. 1D). Interestingly, the occurrence of mosasaur fossils in this outcrop decreases throughout the basal sandstone bed until their disappearance coinciding with the erosive surface (Layer 7 in Fig. 1D). The existence of changes in both facies and fauna associated with the development of a glauconitic interval and an erosive surface is interpreted as an important shift in the palaeoenvironmental conditions in the Maastrichtian section. In this perspective, in-depth foraminifera distribution, stratigraphic, and geochronological analyses are currently underway to refine the stratigraphic framework of these deposits, interpret the palaeoenvironmental conditions associated with the drastic faunal changes, and to approximate the outcrop position within the Mocuio Fm. However, from the fossils recovered above the glauconitic interval (Layers 3–7) (Fig. 1E–H), the occurrence of *Cretalamna maroccana* Arambourg, 1935 (Fig. 1F) suggests a Maastrichtian age (O'leary *et al.* 2019, Guinot and Condamine 2023, Guinot *et al.* 2023). Additionally, possible tooth fragments of *Carcharias heathi* Case and Cappetta, 1997 (Fig. 1G), a species previously reported from the Maastrichtian of the Namibe region, including Bentiaba (Antunes and Cappetta 2002, Costa *et al.* 2019), have also been identified. Fragments possibly belonging to *Chlamydoselachus gracilis* Antunes and Cappetta, 2002 (Fig. 1H), a fossil species also found in the Maastrichtian of Benguela (Antunes and Cappetta 2002), further support this conclusion. Therefore, the specimen analysed here is considered to be Maastrichtian in age.

Phylogenetic analysis methods

Despite the fragmentary nature of the material, sufficient characters could be scored to make informative comparisons. This allowed a dedicated phylogenetic analysis expanding upon the matrices published by Jouve *et al.* (2021). Furthermore, Schwarz *et al.* (2017) have assigned the species *Theriosuchus guimarotae* Schwarz and Salisbury, 2005 to *Knoetschkesuchus guimarotae*, so the latter designation will be used in this study. Analyses were performed employing maximum parsimony approaches, implemented in TNT 1.6 (Morales and Goloboff 2023).

The matrix from Jouve *et al.* (2021) comprises 224 characters, including three continuous characters, and 45 specimens (with the new specimen, MUVP 635 and *Brachiosuchus kababishensis* from Saber *et al.*, 2025 added to the original 42 from the initial study). Of the 224 characters, 43 characters (approximately 20%), including one continuous, could be scored for MGUAN-PA548 (see Supporting Information, Table S1). The analysis parameters have been modified from those used by Jouve *et al.* (2021) since comparable results were achieved using more basic parameters. The following parameters were configured to perform the analysis: Wagner tree with one random seed, 1000 replicates and TBR with 10 trees saved per replication. The best trees obtained were subjected to a final round of TBR branch swapping ('bb' command). The consistency index (CI), retention index (RI), and the Bremer support index were obtained using, respectively, the TNT scripts STATS.RUN and BREMER.RUN included in the TNT software package (v.1.6) (Goloboff *et al.* 2008). The values for absolute bootstrap frequency and GC bootstrap frequency were obtained using the option to resample with the consensus obtained as the base.

The same matrix was subsequently analysed employing Bayesian inference approaches. The continuous characters were transformed into discrete characters following the methods of Jouve *et al.* (2021). We performed a clock analysis, adopting the skyline fossilized birth–death (SFBD) process (Stadler 2010), incorporating tip-dating to estimate divergence times by directly using fossil ages. This allowed us to reconstruct speciation, extinction, and fossilization rates before and after the K–Pg event (66.0 Mya). The relaxed clock model was used to determine independent gamma rates (IGR), with values drawn from a normal distribution function. We placed a soft upper prior in the root to calibrate the tree, and the ages of the tips were modelled according to a uniform prior encompassing their stratigraphic distribution. The latter datum was derived from the Open Access repository Palaeobiology Database (10 November 2024; https://palaeobiodb.org) after occurrences were checked against the associated bibliography. Character evolution followed the Mk model (Lewis 2001) and the values were sampled from a gamma distribution (Supporting Information, Material S1). The analysis was run on the platform CIPRES using MrBayes v.3.2.7a (Ronquist *et al.* 2012), adding a 'dummy' extant taxon to implement the clock analysis. We pruned a posteriori the 'dummy' with the function of 'drop.dummy' from the R-package EvoPhylo (Simões *et al.* 2023) using R v.4.3.0 (R Core Team 2023) and the tree was visualized with FigTree v.1.4.4 (Rambaut 2018) (Supporting Information, Material S2). The convergence of the analysis was assessed using TRACER v.1.7.1 (Rambaut *et al.* 2018), considering the effective sample size (ESS). Furthermore, we assessed the potential scale reduction factor (PSRF) and the average standard deviation of split frequencies (ASDSF) to support the quality of the analysis.

Finally, diversification rates of the tree obtained with the Bayesian inference approaches were analysed using the R-package EvoPhylo (Simões *et al.* 2023) (Supporting Information, Material S3). A 3D model was compiled using Go! SCAN SPARK and the software Vxelements 11.0 (Model 1).

RESULTS

Systematic palaeontology

Crocodylomorpha Hay 1930 (sensuWalker 1970)

Crocodyliformes Hay 1930 (sensu Clark in Benton and Clark 1988)

Mesoeucrocodylia Whetstone and Whybrow 1983 (sensu Benton and Clark 1988)

Tethysuchia Buffetaut 1982 (sensuAndrade *et al.* 2011)

Dyrosauroidea Jouve *et al.* 2021

Dyrosauridae de Stefano 1903

Hyposaurinae Nopcsa 1928

Hyposaurinae indet.

Type horizon and age: Recovered in a marine sandstone (bed 11, Fig. 1D), provisionally associated with a topmost unit of the Mocuio Formation, Maastrichtian (Upper Cretaceous) (Strganac *et al.* 2014).

Type locality: Cemitério de Bentiaba, Municipality of Moçâmedes, Namibe Province, Angola (14°17′05.5′′S; 12°22′34.8′′E).

Material: Posterior portion of the skull including the braincase, right quadratojugal, part of the left ectopterygoid wing, one tooth and bone fragments accessioned as MGUAN-PA548 (Fig. 2).

State of preservation: The specimen comprises an articulated posterior part of the skull, a part of the left ectopterygoid, one tooth, and several small bone fragments (Fig. 2A). The tooth is eroded at its base, but is in good condition, unlike the rest of the material. The exposed and covered bone surface was eroded to a similar degree, precluding the identification of some details of the suture lines. Due to the non-preservation of the entire parietal process, only the base of the process is preserved with a cavity in the centre. In posterior view, the supraoccipital/exoccipital have been severely eroded in their central right side. However, it is possible to observe the posterior part of the parietal, the posterior parts of the squamosal, the supraoccipital, the exoccipitals, part of the basioccipital, the quadrates, and part of the quadratojugals (Supporting Information, Figs S1 and S2).

Description

Parietal (Fig. 2B–D)

The parietal is preserved only by the posterior portion and a part of the interfenestral bar, observable in dorsal view. The poor preservation of the specimen makes the suture lines with the squamosal hard to discern; however, comparison with data in the literature and extant crocodylians allow us to infer that these suture lines are closer to the interfenestral bar than to the lateral margin of the squamosal (Fig. 2D). Both the posterior and the anterior margins of the parietal are strongly eroded, and the posterior one is concave in dorsal view (ch. 90 [1]) (Fig. 2D). The parietal forms part of the posterior margin of the supratemporal fenestrae and creates a thin interfenestral bar dorsally (12-mm wide) (ch. 19 [1], 20 [0], and 25 [2]). The presence of ornamentation on the margins of the supratemporal fenestrae and on the parietal of MGUAN-PA548 cannot be ascertained due to the state of preservation (ch. 21 [1/2] and ch. 93 [3/4]). The posterior margin forms a gently sinuous suture with the supraoccipital and the parietal has a small occipital portion (ch.92 [1] and 96 [0]).

Squamosal (Fig. 2B–E)

Dorsally, the squamosal is anteriorly extended to form part of the skull roof, constituting the posterior region of the supratemporal arch (= upper temporal bar or postorbital-squamosal bar) (Fig. 2D). The preserved supratemporal arch is situated more ventrally than the interfenestral bar, resulting in the cranial table being more convex than horizontal/flat in posterior view (ch. 159 [2]). The squamosal forms a part of the lateral and posterior margin of the supratemporal fenestrae. The margin is large and rounded. The posterior margins of the infratemporal fenestrae are unornamented. The parieto-squamosal transition is hard to recognize because of the poor state of preservation of the specimen. What can be discerned, is that these limits are not in the posteriormost margin of the supratemporal fenestra, but they are closer to the median axis of the cranium (Fig. 2D). The posterior surface of the squamosal is concave in the region lateral to the occipital tuberosities, with the squamosal extending posteriorly to a lesser extent than the occipital condyle (ch. 105 [1] and 107 [0]). In occipital view, the squamosal is also ventrally extended and the suture line with the left exoccipital can be observed running ventrolaterally, exhibiting a sharp prong (ch.103 [1], 104 [1], 106 [1], and 108 [1]) (Fig. 2B). In occipital view, above the occipital tuberosities, the squamosal and the parietal appear to have a small posterior lamina (also visible in dorsal view) that can be associated with the top of the post-temporal canal (Fig. 2B, D). This feature corresponds to character 94 of Jouve *et al.* (2021) described as the 'posterior extension of the parietal'. However, in MGUAN-PA 548, the suture between the squamosal and parietal is unclear due to erosion. To avoid confusion, we will refer to this feature as an extension of the squamosal–parietal region, acknowledging the possibility that, in the studied specimen, the squamosal may also contribute to the extension.

Supraoccipital/exoccipitals (Fig. 2B–D)

The supraoccipital is the most eroded element of the bones preserved in this specimen, and as such, in occipital view, informative morphological details are very difficult to discern. Although, the suture with the exoccipital is eroded, the parietal suture is visible, slightly concave, and gently sinuous ventrally (Fig. 2B). The supraoccipital presents a large hole (due to the preservation), measuring 60 mm wide and 20 mm high. The occipital tuberosities, even though not entirely preserved, are well-developed, widely separated and overhanging by an extension from the squamosal–parietal region (ch. 94 [1] and 120 [2]). However, due to the state of preservation their shape is not clear. The right occipital tuberosity, more developed, is diagonally flattened due to the aforementioned hole on the occipital side. The left tuberosity has a rounded base, but the rest of it is not preserved. It is also unclear whether the occipital tuberosity and the post-temporal fenestra participate in the supraoccipital or not. The paraoccipital processes of the exoccipitals are well preserved, especially the left one. In occipital view (Fig. 2B), the large lateral suture of the left contact with the squamosal can be observed well, while the right one can only be inferred due to erosion (ch. 122 [1]). The paroccipital processes of the exoccipitals are ventrally directed along the quadrate, and they end with rounded and well-developed processes at the same

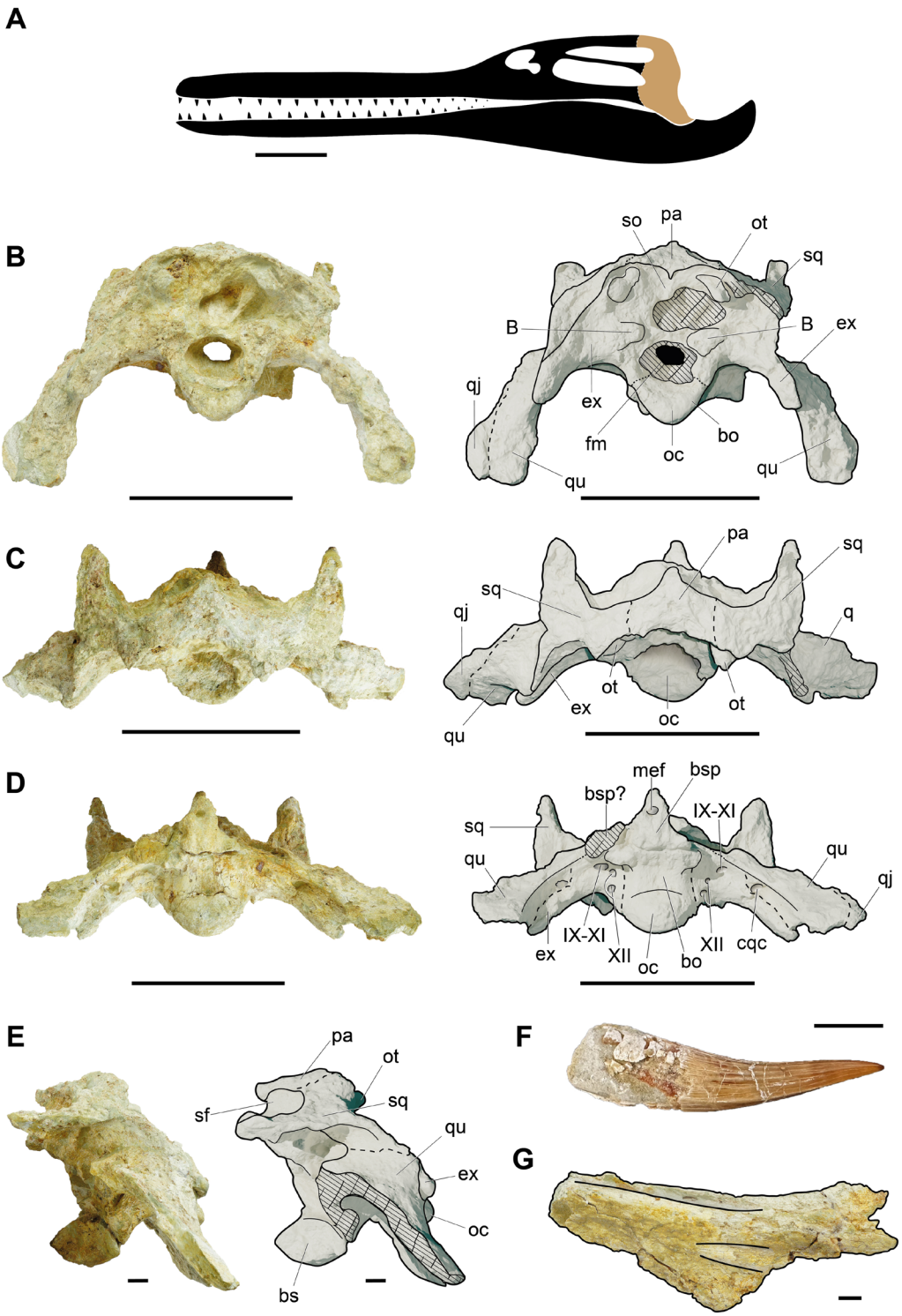

Figure 2. Cranial remains of MGUAN-PA548: superimposed on skull outline from Jouve *et al.* (2006) (A); the skull (photography and 3D model views): in posterior view (B), in dorsal view (C), in ventral view (D), in left lateral view (E); tooth in lingual view (F); part of the left ectopterygoid wing (G); (additional views of the specimen are available in the Supporting Information, Material S6, S7). Abbreviations: B, boss; bo, basioccipital; bsp, basisphenoid; cqc, cranioquadrate canal foramen; ect, ectopterygoid; ex, exoccipital; fm, foramen magnum; mef, median eustachian foramen; q, quadrate; qj, quadratojugal; oc, occipital condyle; ot, occipital tuberosity; pa, parietal; pop, paroccipital process; pt, pterygoid; so, supraoccipital; sq, squamosal; stf, supratemporal fenestra; IX, glossopharyngeal nerve; X, vagus nerve; XI, accessory nerve; XII, anterior and posterior bundles of hypoglossal nerve. Scale bar = 10 cm (A–D) and 1 cm (E–G).

level as the occipital condyle (ch. 119 [1]). The suture between the exoccipital and basioccipital is partially discernible, allowing for an approximate placement on the occipital condyle but the exoccipital largely participates (ch. 118 [0]). In ventral view, the exoccipitals do not bear any crest or ornamentation (ch. 123 [0] and 124 [0]). In occipital view, the foramen magnum is symmetrically flanked by two rounded structures positioned laterally and slightly dorsally (Fig. 2B). These bony projections, referred to here as bosses, measure approximately 15 mm in diameter and exhibit an occipital projection of just under 5 mm.

Basioccipital (Fig. 2B, D)

The basioccipital is 26 mm long anteroposteriorly, 37 mm wide lateromedially and shows a depression on the ventral surface (ch. 129 [1]). In occipital view, MGUAN-PA548 presents a 'V'-shaped morphology (tipping ventrally), and the occipital condyle is twice as wide as it is high (ch. 2 [2]). The posterior surface of the main body of the basioccipital below the condyle is not vertical; it is inclined, faces posteroventrally, and is visible in posterior view (ch. 132 [1]).

Basisphenoid (Fig. 2C)

Only the posteriormost part of the basisphenoid is preserved. The medial 7 ustachian foramen is present, well visible in ventral view but not in occipital view (ch. 127[0]). Only the contact with the basioccipital has been preserved. A small fragment of the basisphenoid is also preserved and is placed to the right of the central block of the basisphenoid.

Quadrate (Fig. 2B–E)

The quadrate is very long, almost flattened, directed posteroventrally (very verticalized), and sutured completely laterally with the squamosal (ch. 135 [2], 136 [0], 140 [1], and 141 [2]). Both the right and left quadrates are well-preserved, their suture lines with the exoccipitals are straight, and their condyles extend further ventrally than the occipital condyle (ch. 139 [1]). Contact with the squamosal is made along the posterior wall of the supratemporal fenestra, ventrally and laterally to the presumed location of the temporal canal. The quadrate has no ornamentation, and its entire surface is smooth. Only a small portion of the left quadratojugal is preserved and follows the same orientation as the quadrate. Lastly, the posterior margin of the infratemporal fenestra is posterior to the supratemporal fenestra margin (ch. 29 [1]).

Foramen magnum (Fig. 2D)

Although its limits are severely eroded, the foramen magnum is located above the occipital condyle with a similar diameter as the latter in occipital view. In anterior view, the diameter of the foramen is reduced by half, forming a conical hole. In ventral view, it is possible to distinguish different foramina, here identified as: the foramen of the anterior bundle of the hypoglossal nerve (Fig. 2D—XII), the foramen of the posterior bundle of the hypoglossal nerve (Fig. 2D—XII), the cranioquadrate canal foramen (Fig. 2D—cqc), the foramen of the glossopharyngeal nerve (Fig. 2D—IX), the foramen of the vagus nerve (Fig. 2D—X), the foramen of the accessory nerve (Fig. 2D—XI) and the median 8 ustachian foramen (Fig. 2D—mef). All these foramina have been named and identified following the nomenclature of Erb and Turner (2021). The first four foramina border the basisphenoid laterally (ch. 133 [0]). In ventral view, the medial 8 ustachian foramen is situated anterior to the posterior margin of the supratemporal fenestra (ch. 134 [1]). In the same view, it is possible to identify the cranioquadrate canals, which are hidden in occipital view by the exoccipital (ch. 131 [1]). These canals are positioned on the ventral side of the quadrate, just at the beginning of the exoccipital tuberosities. The temporal canals are filled with sediment and are indistinguishable in anterior view; however, an iron spot on the left side may indicate the position of the left temporal canal.

Isolated material (Fig. 2F, G)

Some elements have been excavated from the same block of the skull and are interpreted as part of the same specimen. A fragment of the left ectopterygoid has been recognized (Fig. 2E). The fragment is straight anteroposteriorly and slightly concave dorsoventrally. The fragment thickens posteriorly and forms a process that separates it into two distinct parts. The dorsal part bears a 5-mm diameter slit on the left lateral side that gradually fades from the posterior half of the fragment. In addition, the dorsal side has a ridge parallel to the previous slit starting at the posterior half of the fossil. One isolated tooth was collected (Fig. 2F), measuring 42 mm in crown height, 10 mm in crown base mesiodistal length, and 5 mm in crown base labiolingual width. It exhibits an elliptical cross-section, featuring straight carinae devoid of serrations, with the enamel displaying a dozen pronounced ridges, in particular on the lingual side of the tooth (ch. 196 [1], 197 [0], and 198 [0]).

Phylogenetic analysis

Maximum parsimony analysis

The consensus was obtained from 144 trees proposing a tree length of 821.338 steps with a consistency index of 0.385 and a retention index of 0.743 (Fig. 3). The topology of the cladogram obtained is identical to the one of Jouve *et al.* (2021) with the well-supported node Tethysuchia (absolute bootstrap frequency of 87) split in two lineages: Pholidosauridae and Dyrosauroidae. This node is supported by 16 unambiguous synapomorphies (ch: 4 [1], 6 [2], 40 [1/2], 51 [0], 59 [1], 62 [1], 70 [1], 104 [1], 125 [1], 149 [1], 163 [2], 164 [2], 166 [1], 168 [1], 179 [1], and 192 [1]).The clade Dyrosauridae highlighted an absolute bootstrap of 56 with 40 unambiguous synapomorphies (ch: 2, 3, 8 [1], 11 [2], 14 [1], 17 [3], 18 [0], 29 [1], 39 [1], 43 [1], 44 [0], 45 [1], 54 [1], 55 [1], 56 [0], 59 [0], 63 [0], 67 [1], 70 [0], 71 [1], 81 [1], 85 [0], 90 [2], 102 [2], 114 [0], 115 [1], 118 [1], 119 [1], 120 [1/2], 122 [1], 124 [0], 139 [1], 140 [1], 142 [1], 148 [1], 159 [1], 162 [0], 169 [1], 186 [1], 193 [1], and 196 [1]). As for Hyposaurinae, five unambiguous synapomorphies and an absolute bootstrap of 21 (ch: 4 [2], 36 [1], 42 [1], 67 [0], and 194 [1]). The strict consensus places the specimen MGUAN-PA548 in a polytomy with *Luciasuchus* (Jouve *et al.* 2021), *Dyrosaurus* spp. and a large group of Hyposaurinae. The polytomy is supported with only one unambiguous synapomorphy (ch. 198 [0]). MGUAN-PA 548 is supported by a unique combination of characters: the occipital condyle much wider than high (ch. 2 [2]) and the parietal without broad occipital portion (ch. 96 [0]). Within

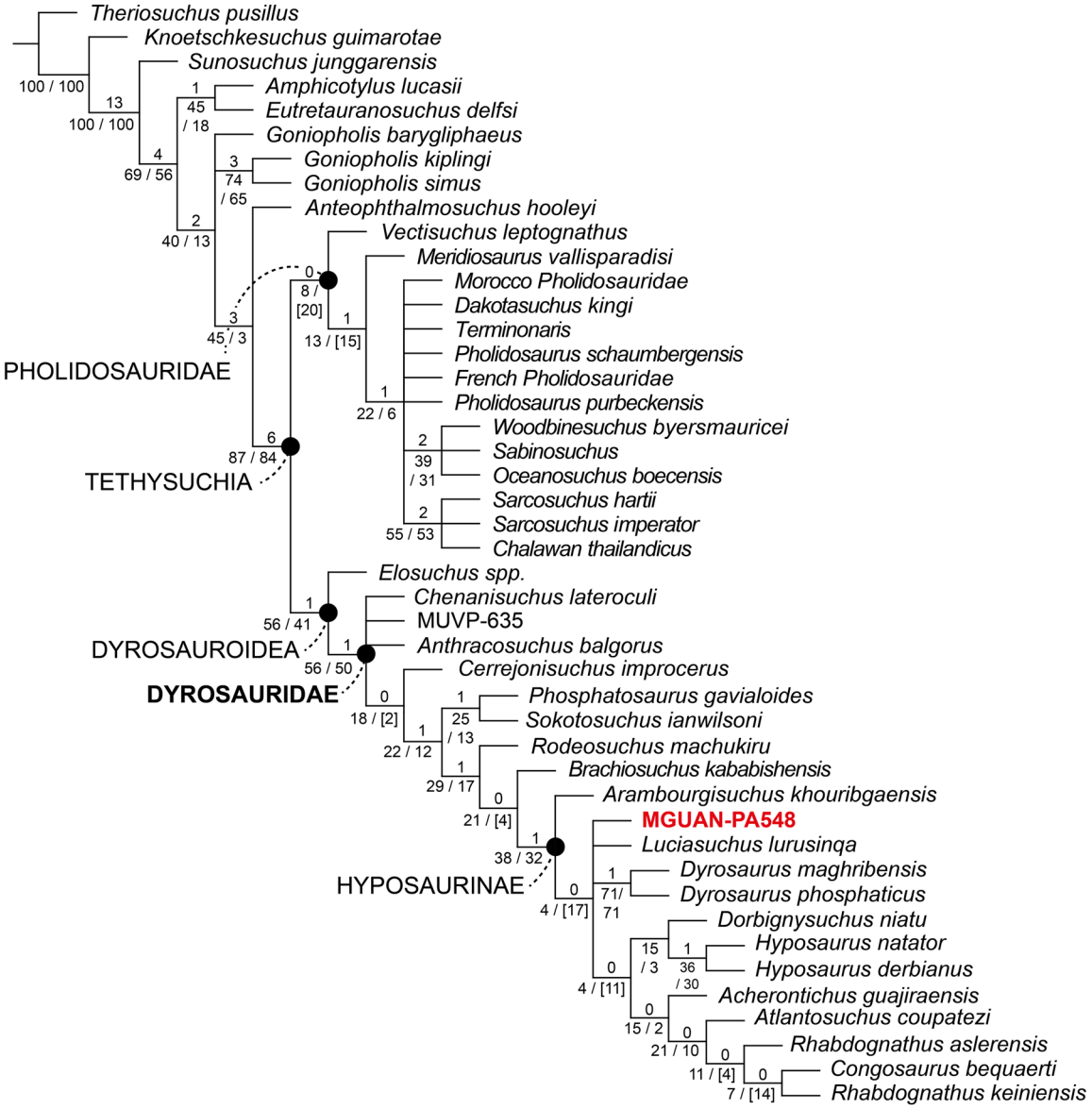

Figure 3. Strict consensus tree of 336 most parsimonious trees of phylogenetic analysis on TNT (CI = 0.385; RI = 0.743; L = 821.338) of Jouve *et al.* (2021) matrix with the addition of MGUAN-PA548. Branch supports are Bremer support, absolute bootstrap frequency and GC bootstrap frequency, with negative values between brackets.

the Hyposaurinae lineage, only the genus *Dyrosaurus* is supported with a bootstrap higher than 71. Although well resolved, the tree does not appear to be stable (low bootstrap frequencies), as can be seen for the whole tree outside the well-defined clades described above.

Bayesian inference

The Bayesian analysis reached convergence for each parameter (ESS > 200), and the good quality of the analysis is supported by PSRF = 1.000 and ASDSF = 0.005345. In the maximum compatibility tree (MCT), the major clades are supported with high posterior probabilities, i.e. Tethysuchia (PP = 0.89), Dyrosauridae with MHNM-kh01 (PP = 0.74), and Hyposaurinae (PP = 0.80) (Fig. 4). However, within these taxa, the viability of the results decreases with posterior probabilities close to or below 0.5. This is particularly the case in the complex in which specimen MGUANPA-548 is placed. The complex, which includes species from the genera *Rhabdognathus*, *Congosaurus* (Dollo 1914), *Atlantosuchus* (Buffetaut and Wouters 1979), and *Acherontisuchus* (Hastings *et al.* 2011), along with the specimen analysed in this study, trends toward a posterior probability of 0.26. However, as the phylogenetic relationships among these taxa become more clearly defined, this posterior probability decreases further. Only the two species of the genus *Rhabdognathus* (Swinton 1930) have higher posterior probabilities (PP = 0.56). Identical observations are recognized with the maximum parsimony analysis, major clades exhibit stronger support with bootstrap values exceeding 50 [i.e. Tethysuchia (BS = 87), Dyrosauroidea (BS = 56), and Dyrosauridae (BS = 56) (Fig. 3)]. However, the MCT topology presents some differences with the strict consensus tree of maximum parsimony analysis. First, the tree is divided into two major clades: Tethysuchia and Goniopholididae. Second, Dyrosauroidea

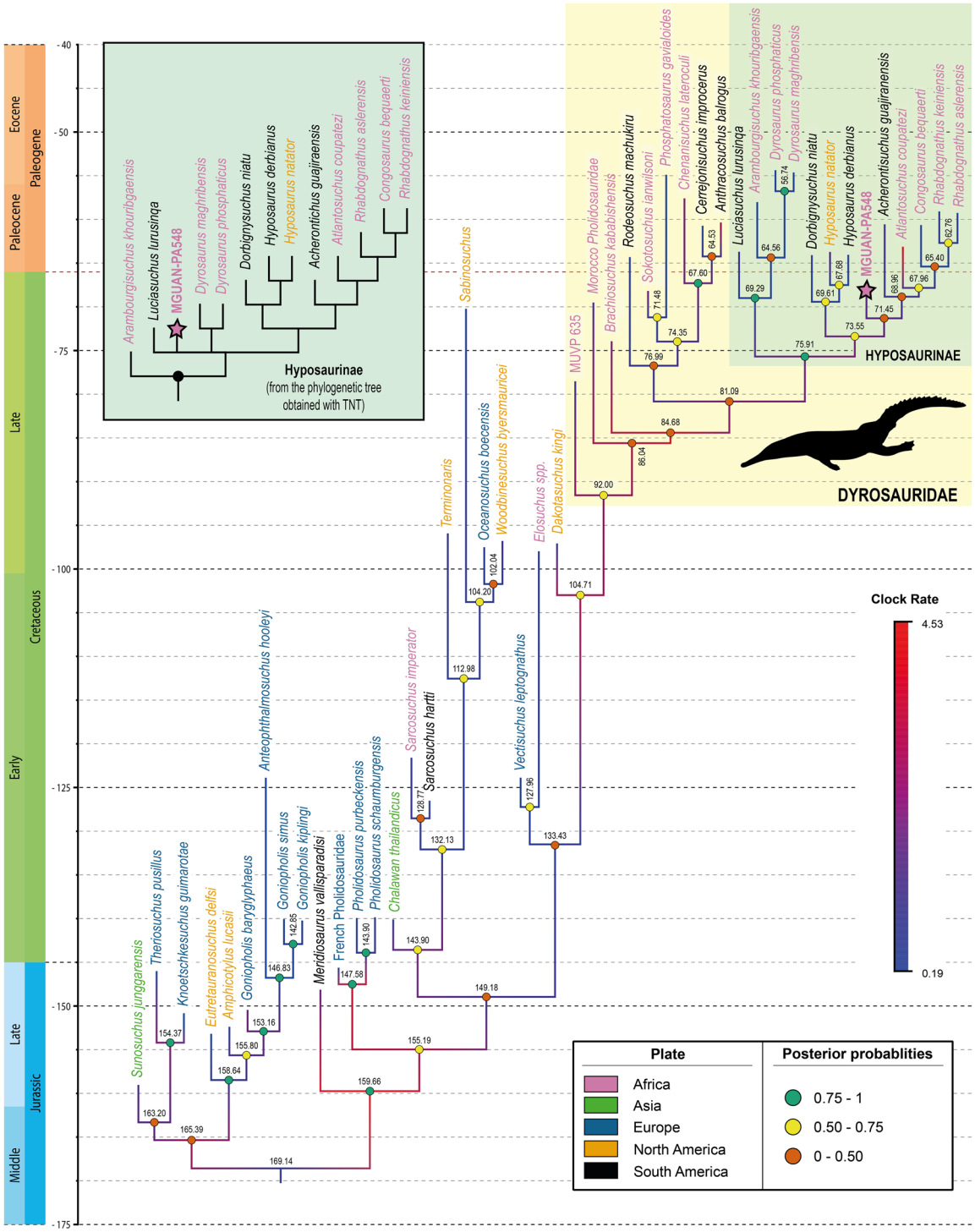

Figure 4. Tip-dated maximum compatibility tree (MCT) of the Bayesian clock analysis. Silhouette of *Guarinisuchus munizi* by Nobu Tamura, vectorized by Zimices available on PhyloPic.

is included within Pholidosauridae and not two different branches like the maximum parsimony topology. Within the dyrosaurids, the tree topology is quite similar: the branch of *Hyposaurus* (Owen 1849) and *Dorbignysuchus* (Jouve *et al.* 2021) is placed as the sister-lineage to *Rhabdognathus* (Fig. 4). The polytomy with MGUANPA-548 is resolved and the hyposaurine are divided in two branches with the first one including *Dyrosaurus* species, *Luciasuchus*, and *Arambourgisuchus* (Jouve *et al.* 2005b).

However, the change of placements of *Brachiosuchus kababishensis* (as one of the earliest Dyrosauridae) and *Chenanisuchus lateroculi* Jouve *et al.*, 2005a (as sister-taxa of *Cerrejonisuchus improcerus* Hastings *et al.*, 2010 and *Anthracosuchus balgorus* Hastings *et al.*, 2015 with a posterior probability of 0.99) are notable. Nonetheless, as for clock rates, the whole tree shows rather low rates (clock rates < 1), but it is possible to distinguish two events of strong morphological change (clock rates > 2). The first occurs

at the base of the Tethysuchia during the Jurassic, associated with the first Pholidosauridae, and the second from the Aptian to the Campanian, covering the entire origin of the Dyrosauridae lineage. There is also a high rate of occurrence at the origin of the taxon *Atlantosuchus coupatezi* Buffetaut and Wouters, 1979.

Diversification rates

Our data do not follow the theoretical normal distribution for each time bin and parameter (see Fig. 5; Supporting Information, Table S2; Shapiro–Wilk test, all *P*-values <0.05). Because the data do not follow a normal distribution, the Student *t*-test will not be used to analyse the result. The speciation and extinction parameters of the two time bins (before and after 66.0 Mya) remain different and are supported by *P*-values below 0.05, as determined by Bartlett's and Mann–Whitney U-test (Fig. 6; Supporting Information, Table S2). For the speciation and extinction parameters, the Fligner–Killeen and Bartlett test does support homoscedasticity with a *P*-value below 0.05. Despite this, the relative fossilization results from the tests (excluding Shapiro–Wilk) are associated with *P*-values of 0 (Fig. 6; Supporting Information, Table S2). Despite the questionable zero value, there seems to be a clear fossilization bias between the two time bins (before and after the K–Pg event, an aspect discussed later).

Estimated size

The absence of a complete cranium makes it difficult to reconstruct the overall size of the specimen. Nevertheless, based on the results of phylogenetic analyses, MGUAN-PA548 is close to the genera *Luciasuchus*, *Acherontisuchus*, *Atlantosuchus*, *Rhabdognathus*, and *Congosaurus*, and as such is considered to be an elongated and slender-snouted crocodylomorph (Jouve and Schwarz 2004, Jouve 2007, Jouve *et al.* 2008). In 2022, Salih *et al.* estimated the size of *Rhabdognathus keiniensis* Jouve, 2007 as between 4.72 and 5.44 m. The posterior width of the holotype of the species *Rhabdognathus keiniensis* (MNHN TGE 4031; Jouve 2007; Fig. 8) exhibits a similar size range to MGUAN-PA548 (MNHN TGE 4031 ≈ 213 mm, based on the figure 9.2 in Jouve 2007, MGUAN-PA548 = 219 mm). Thus, we estimate the size of the Angolan individual also close to 5 m.

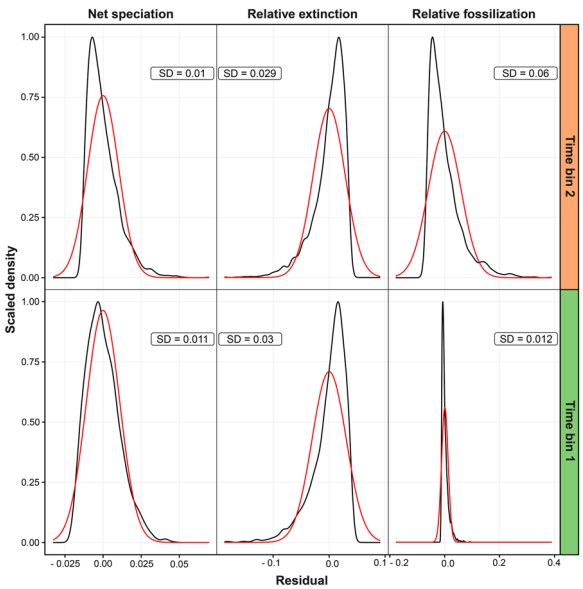

Figure 5. Visualization of deviations from normality for each diversification parameter in the FBD model for the two time bins base on the Bayesian time-calibrated tree.

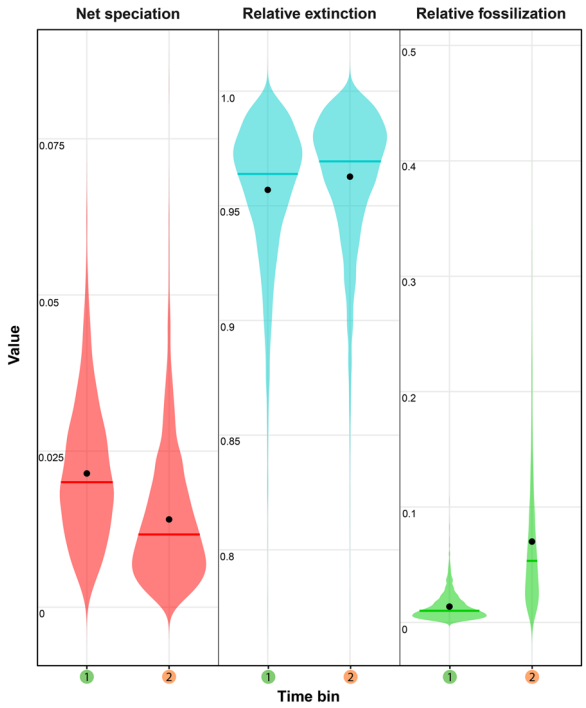

Figure 6. Visualization of posterior estimates for each diversification parameter in the FBD model for the two time bins base on the Bayesian time-calibrated tree.

DISCUSSION

Comparison

Despite the fragmentary nature of the material, the diagnosis by Jouve *et al.* (2006) allows MGUAN-PA548 to be attributed to Dyrosauridae. The posterior part of the skull presents the following diagnostic characters: occipital tuberosities directed posteriorly formed by the exoccipitals, exoccipital participates considerably in the occipital condyle (ch. 118 [1]), and lateral Eustachian foramen located dorsal to the medial Eustachian foramen (ch. 131 [1]).

Here, MGUAN-PA548 will be compared to Hyposaurinae as defined by Nopcsa (1928). Fittingly, the elongated and fine morphology of the isolated tooth seems to correspond with Buffetaut's (1980) definition of this taxon as dyrosaurids with narrow snouts and long, sharp teeth. However, the genus *Congosaurus* is defined by the species *Congosaurus bequaerti*, but none of its diagnostic characters are applicable to MGUAN-PA548: the holotype of the species lacks the posterior part of the skull. The same conclusion is applicable for its sister-taxon *Congosaurus compressus* Buffetaut, 1980. Therefore, there is no direct comparison between the fossil described here and the genus *Congosaurus*. The same is true for the genus *Luciasuchus* and its type species *Luciasuchus lurusinqa* and for *Acherontisuchus* (Hastings *et al.* 2011) and its type species *Acherontisuchus guajiraensis* Hastings *et al.*, 2011. Thus, comparisons will be made with the relevant material below. However, it is

notable that *Luciasuchus* and *Congosaurus* present identical tooth morphology.

The newly described *Brachiosuchus kababishensis* by Salih *et al.* (2022) differs from MGUAN-PA548, although the state of preservation of both specimens is poor, in having its occipital tuberosities less developed (ch. 120 [1]) and the supratemporal fenestrae posterior walls being more dorsally inclined (ch. 20 [1]). Additionally, in occipital view, the exoccipital does not bear any crest and the overall skull roof in occipital view is more convex on MGUAN-PA548 (ch. 123 [0] and 159 [2]).

MGUAN-PA548 does not belong to the monospecific genus *Arambourgisuchus*, with the species *Arambourgisuchus khouribgaensis*, according to its diagnosis. Indeed, MGUAN-PA548 can be excluded due to the presence of occipital tuberosities overhanging the posterior extension of the parietal (ch. 94 [1]) and the posterior edge of the supratemporal fenestra being much larger in *Arambourgisuchus* (ch. 19 [2]). Furthermore, the parietal does not extend occipitally and does not have a strong and acute process in the occipital face, between the occipital tuberosities, when viewed dorsally (*Arambourgisuchus*—ch. 90 [4], 96 [1]). In occipital view, the ventral part of the basioccipital in *Arambourgisuchus* is visible and vertical (ch. 132 [1] and 134 [0]). Finally, like *Brachiosuchus kababishensis*, the overall skull roof in occipital view is clearly more convex on MGUAN-PA548 (ch. 159 [2]).

In contrast to the description provided by Jouve *et al.* (2006) for *Dyrosaurus* (Pomel, 1894), MGUAN-PA548's interfenestral bar is thinner and upside-down V-shaped (ch. 25 [2] and 27 [2]). The parietal differs quite a lot, for *Dyrosaurus* specimens the posterior margin is straight and the suture with the supraoccipital forms a 'w'-shape, rather than being sinuous (ch. 90 [2] and 92 [2]). In occipital view for *Dyrosaurus*, the parietal presents a large occipital portion (ch. 96 [1]). The occipital tuberosities are not overhung by any posterior extension of the parietal (94 [0]). Additionally, laterally to these tuberosities, the posterior margin of the squamosal is straight in dorsal view (ch. 105 [0]). Moreover, MGUAN-PA548 does not exhibit paired grooves along the ventral surface of the basioccipital, as in *Dyrosaurus* (ch. 130 [0]). Furthermore, this portion of the basioccipital is inclined and not visible in occipital view (ch. 132 [2] and 134 [1]).

Defined by Jouve *et al.* (2021), the genus *Dorbignysuchus* is represented by a single species *Dorbignysuchus niatu* Jouve, de Muizon, Cespedes-Paz, Sossa-Soruco and Knoll, 2021 known from three Palaeocene specimens found in Bolivia. MGUAN-PA548 shares two diagnostic characters with this genus: (1) narrow interfenestral bar; and (2) extension of the squamosal-parietal region above the occipital tuberosity. However, MGUAN-PA548 differs in that the parietal does not have a broad occipital portion (ch. 96 [0]), the squamosal does not project posteriorly beyond the occipital condyle (ch. 107 [0]) and lastly, like *Dyrosaurus*, the basioccipital is inclined and not visible in occipital view (ch. 132 [2] and 134 [1]).

The validity of the genus *Hyposaurus* is disputed due to a diagnosis based on two isolated vertebrae, a specimen associated with *H. rogersii* Owen, 1849 and later as a nomen dubium by Norell and Storrs, 1989 (Jouve *et al.* 2021). Furthermore, the holotype of *H. derbianus* Cope, 1885 does not present material that can be compared to MGUAN-PA548. In addition, the species *Guarinisuchus munizi* Barbosa *et al.*, 2008 was interpreted by Jouve *et al.* (2021) as a possible *H. derbianus*. Thus, in the absence of a complete and valid diagnosis, the comparison of MGUAN-PA548 to the genus was based on the matrix of Jouve *et al.* (2021) and on the specimen NJSM 10416 identified as *H. rogersii* by Denton *et al.* (1997), the specimen NJSM 23368 identified as *H. rogersii* by Callahan *et al.* (2015), the specimen DG-CTG-UFPE 5723 identified as *G. munizi* in the study by Barbosa *et al.* (2008) and re-evaluated as *H. derbianus* by Jouve *et al.* (2021), and the specimen Cat. No. 985, Y.P.M. (YPM 985) identified as *H. natator* Troxell, 1925.

For NJSM 23368 and NJSM 10416 (*H. rogersii*), MGUAN-PA548 exhibits distinctive morphological features. The two specimens present a larger occipital condyle (ch. 2 [1]), and a squamosal that projects further posteriorly than the occipital condyle (ch. 107 [1]). In comparison to MGUAN-PA548, DG-CTG-UFPE 5723 (*H. derbianus*) stands out with several distinctive features: it is notably bigger in size; possesses relatively larger exoccipital processes in relation to the quadrate; lacks a posterior elongation of the squamosal; and exhibits more pronounced occipital tuberosities, although they are also covered dorsally by the extension of the squamosal-parietal region and the squamosal is also slightly curved.

The fossil YPM 985 (*Hyposaurus natator* holotype) has a limited amount of comparable material (quadrate, quadratojugal, and part of the squamosal) with MGUAN-PA548. However, the matrix of Jouve *et al.* (2021) enabled us to compare it with *H. natator*. Although the occipital condyle is more flattened, *H. natator* shares the same distinguishing features as its counterpart, to which the following can be added: the absence of a posterior extension of the squamosal–parietal region (ch. 94 [0]); a parietal with a large occipital portion (ch. 96 [1]); a straight posterior margin of the squamosal (ch. 105 [0]); and the presence of paired grooves on the surface of the basioccipital (ch. 130 [0]). Lastly, it is noteworthy that *H. natator* displays distinct teeth, characterized by a twisted carina and smooth enamel (ch. 196 [1] and 197 [1]).

For the monospecific genus *Atlantosuchus* (known by a single specimen, *A. coupatezi* Buffetaut and Wouters, 1979), the diagnosis of Jouve *et al.* (2008) does not present any diagnostic characters applicable to MGUAN-PA548. However, MGUAN-PA548 differs in having a posterior margin of the parietal much less concave anteriorly (ch. 90 [1]) and does not have a large occipital portion (ch. 96 [0]). The occipital condyle is flatter (ch. 2 [2]) and the squamosal does not project further posteriorly (ch. 107 [0]). In *Atlantosuchus*, the suture between the parietal and supraoccipital is more sinuous (ch. 92 [2]). Furthermore, although only the posterior base of the interfenestral bar of MGUAN-PA548 is preserved, it does not appear as thick as in *A. coupatezi* (ch. 25 [1]).

MGUAN-PA548 exhibits several features used as diagnostic characters of the genus *Rhabdognathus* given by Jouve (2007): (i) lateral arches of supratemporal fenestra (= upper temporal bar or postorbital–squamosal bar) and interfenestral bar are very thin, although non-ornamentation cannot be confirmed; (ii) large distance between posterior limit of occipital condyle and medial eustachian foramen; (iii) occipital tuberosities long, well-developed and widely spaced; (iv) weak participation of parietal in occipital surface (parietal dorsoventrally narrow), and suture with supraoccipital gently sinuous ventrally (not W-shaped).

MGUAN-PA548 indeed aligns with some diagnostic features of the genus *Rhabdognathus* but it can be distinguished from *Rhabdognathus keineinsis* (Jouve 2007) by several key features: (i) the space between the occipital tuberosities is much less concave anteriorly in MGUAN-PA548; (ii) the occipital tuberosities themselves are less developed compared to *R. keineinsis*; and (iii) the posterior shape of the parietal in MGUAN-PA548 is only slightly concave, an aspect similar to *Rhabdognathus aslerensis* Jouve, 2007. However, it also exhibits differences from *R. aslerensis*, including: (i) more developed exoccipital processes in MGUAN-PA548, which extend to approximately halfway up the quadrate; (ii) the exoccipital and quadrate in MGUAN-PA548 extend further laterally than the squamosal; and (iii) there is no posterior elongation of the squamosal in MGUAN-PA548.

Compared with the previously mentioned taxa, MGUAN-PA548 presents an intermediate morphology in dorsal view between *R. keineinsis* and *R. aslerensis* revealing a unique combination of characters (Fig. 7): (i) undeveloped squamosal process posteriorly, and (ii) a posterior shape of the parietal slightly concave (Fig. 7). MGUAN-PA548 presents a distinctive combination of homoplasy of characters of other Hyposaurinae: thin occipital condyle; well-developed exoccipital tuberosities with a large suture with the squamosal; and presence of an extension of the parietal overhanging the occipital tuberosities. Furthermore, MGUAN-PA548 reveals a unique distinctive trait (autapomorphy): the presence of two rounded bosses placed symmetrically on the laterodorsal sides of the foramen magnum in occipital view.

Systematic affinities

The strict consensus analysis places MGUAN-PA548 in a basal polytomy weakly supported with other hyposaurines (BB = 4), including *Luciasuchus lurusinqa*, *Dyrosaurus* spp., and a clade encompassing the majority of hyposaurines (Fig. 3). Similar results are obtained with the Bayesian analysis, with the specimen

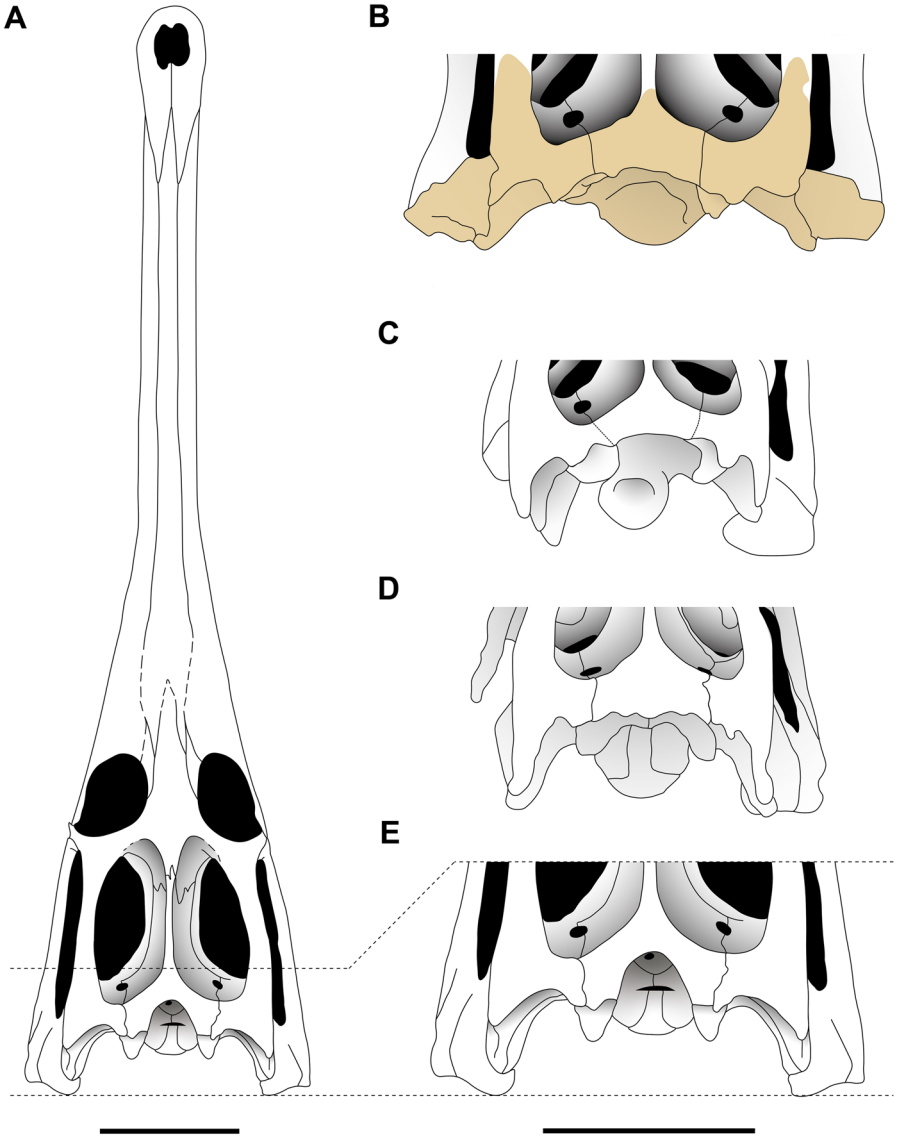

Figure 7. *Rhabdognathus keiniensis* skull in dorsal view (A) and distal parts of the skull of Dyrosauridae in dorsal view: of MGUAN-PA548 (B), DG-CTG-UFPE 5723 (C), *Rhabdognathus aslerensis* holotype (MNHN TGE 4031) (D), *Rhabdognathus keiniensis* holotype (CNRST-SUNY_190) (E), modified from Jouve (2007). Scale = 10 cm.

placed within the Hyposaurinae lineage, basal to the *Rhabdognathus* species, *Congosaurus bequaerti*, *Atlantosuchus coupatezi*, and *Acherontichus guajiraensis*, although with limited support (PP = 0.26). The Hyposaurinae node is well-supported in the tip-dated MCT (PP = 0.81), in contrast to the strict consensus topology (BB = 38). This pattern extends more broadly within Hyposaurinae, where, apart from the *Dyrosaurus* spp. node, no node exceeds a bootstrap value of 38. In comparison, the Bayesian analysis appears to more effectively resolve parent relationships. The temporal calibration of species, therefore, appears to be an important factor in resolving phylogenetics links. Based on the relative stratigraphic position and assigned to the Maastrichtian, MGUAN-PA548 is placed consequently in a basal position relative to the Palaeogene taxa.

Therefore, it is important to highlight that the Cretaceous fossil discoveries of Hyposaurinae are not included in the matrix. A fragmentary Hyposaurinae indet. from Mali, initially described as *Rhabdognathus keiniensis*, was considered Maastrichtian in age (Hill *et al.* 2008, Jouve *et al.* 2021). Additionally, an Upper Cretaceous specimen from Sudan, originally identified as *Hyposaurus* sp., has been reassigned to Hyposaurinae (Salih *et al.* 2016, Jouve *et al.* 2021).

The appearance and diversification of Hyposaurinae are considered to have occurred during the late Campanian (75.91 Mya) and Maastrichtian, as suggested by the tip-dated MCT (Fig. 4). The Malian and Sudanese specimens could, therefore, serve as evidence, supporting the hypothesis proposed by Jouve and Jalil (2020), Jouve *et al.* (2021), and Jouve (2021), which suggests that Dyrosauridae underwent significant diversification during the Maastrichtian, expanding their range across the Atlantic Ocean from Africa to South America. In this context, the Angolan specimen MGUAN-PA548 represents one of the earliest pieces of evidence for this trans-Atlantic dispersal and subsequent diversification along the southern African coast.

If we compare our results to the phylogeny of Hastings *et al.* (2010, 2011, 2015), calibrated in stratigraphic and geographic contexts, our outcomes are similar. Although the matrix of Hastings *et al.* (2011) is less complete and its topology is not well resolved, the two groups of Hyposaurinae and non-Hyposaurinae are found. The hypothesis of diversification and migration toward the Southern Hemisphere during the Maastrichtian, proposed by Hastings *et al.* (2010, 2011, 2015), is further supported by the new discovery from Angola.

Notably, *Brachiosuchus kababishensis*, described from an Upper Campanian–Maastrichtian strata, is recovered in the Bayesian analysis as one of the most basal Dyrosauridae, like the results from Hastings's matrix in Salih *et al.* (2022). This contrasts with the findings of Saber *et al.* (2025), where *B. kababishensis* is placed closer to Hyposaurinae, as in the strict consensus analysis, where it is positioned as a sister-clade to Hyposaurinae. In this paper, *B. kababishensis* is not considered Hyposaurinae, although it could fit the definition provided by Jouve *et al.* (2021): 'This is the crown clade including the species more closely related to *Dorbignysuchus niatu*, *Dyrosaurus* spp., and *Hyposaurus* spp. than to *Rodeosuchus machukiru* and Phosphatosaurinae'. This taxonomic uncertainty was previously highlighted by Saber *et al.* (2025), emphasizing the need for further research and discoveries to clarify the species' placement. Additionally, this Bayesian finding aligns with the hypothesis that north-eastern African fauna played a significant role in the emergence and diversification of Dyrosauridae, an aspect highlighted by Saber *et al.* (2025). These authors suggest that this evolutionary process probably initiated during the Coniacian–Santonian, although our findings supported by Bayesian analysis suggest this process could have occurred earlier, within the Turonian (~92.00 Mya).

In the phylogenetic analysis, MGUANPA-548 is classified as Hyposaurinae despite lacking a complete mandible. The observation of the mandible plays a crucial role in diagnosing certain genera within the clade. For example, a key distinguishing feature between *Rhabdognathus* and *Hyposaurus* lies in mandibular morphology, particularly the shape of the symphysis. In *Rhabdognathus*, the symphysis is as wide as it is high or even taller, whereas in *Hyposaurus*, it is consistently wider than it is high. This characteristic contributed to the reclassification of *G. munizi* as *Hyposaurus*, as noted by Jouve *et al.* (2021). Furthermore, *Congosaurus*, *Acherontisuchus*, and *Luciasuchus* lack overlapping diagnostic features or material consistent with MGUANPA-548. While localities align with those of *Congosaurus bequaerti* (Palaeocene, Angola), it is worth noting that the diagnosis of this genus is primarily based on snout characteristics. Furthermore, the validity of *Congosaurus* has been extensively debated, with some discussions suggesting it may be synonymous with the genera *Hyposaurus* and *Rhabdognathus* (Jouve and Schwarz 2004). Consequently, in the absence of preservation of mandibular material, the hypothesis that MGUAN-PA548 is closer to the genera *Luciasuchus*, *Acherontisuchus*, *Congosaurus*, or *Hyposaurus* cannot be completely ruled out. Ultimately, resolving the taxonomy of MGUAN-PA548 and reassessing the validity of *Luciasuchus*, *Acherontisuchus*, *Congosaurus*, and *Hyposaurus* would greatly benefit from the discovery of new material and from a thorough revision of American dyrosaurid fossils. Such efforts are crucial for advancing our understanding of these ancient reptiles and their evolutionary relationships.

Nevertheless, despite MGUAN-PA548 displaying a unique combination of features, the material remains too fragmentary to confidently assign the specimen to any currently recognized genus or to diagnose it as a new species. The absence of a complete mandible, a key element in dyrosaurid taxonomy, significantly limits the resolution of its taxonomic status. Morphological comparisons, as well as both maximum parsimony-based and Bayesian phylogenetic analyses, do not provide conclusive support for assigning MGUAN-PA548 to a new species. Consequently, we consider the specimen as Hyposaurinae indet.

Macroevolution of Hyposaurinae

The diversification rate analysis using the EvoPhylo package indicates a notable shift in the speciation and extinction patterns of Dyrosauridae before and after the K–Pg event, as suggested by Jouve in 2021. However, this conclusion is not supported statistically, with the non-normal distribution of the data caused by the fossilization bias (the large majority of Hyposaurinae have been recovered from the Palaeocene, and only a few before the K–Pg) or by the utilization of a 'dummy' taxon. Indeed, calibrated in the Bayesian analysis to time zero, the range of the 'dummy' taxon

extends over more than 200 M.y., so it will have an impact on the extinction parameter.

Accordingly, drawing conclusions exclusively from diversification rates seems inappropriate. The discovery of Campanian/Maastrichtian fossil material or the use of other methods is, therefore, required to properly calibrate and assess these rates. The results and conclusions assessed by Jouve (2021), such as aquatic longirostrine crocodyliforms diversifying at the end of the Cretaceous and Early Palaeocene with a marked diversification of crocodyliforms after the K–Pg event, have been identified with the R-package EvoPhylo. However, this result could, therefore, reflect an important fossil bias. The diversification of Hyposaurinae would indeed have occurred during the Maastrichtian, as supported by our Bayesian phylogeny, and the strong diversification by the beginning of the Palaeogene, but the latter hypothesis would not be supported statistically and would be an artefact of a fossilization bias. The recent study of Payne *et al.* (2024) showed that the speciation rates, extinction rates and overall diversity of tethysuchians and gavialoids were unaffected by the Cretaceous/Palaeogene mass extinction. However, this does not preclude a gradual diversification of dyrosaurids during the Maastrichtian and Palaeocene, as suggested in Jouve (2021) and Jouve and Rodríguez-Jiménez (2023). As presented by Rio and Mannion (2021), the peak in marine reptile diversity was attained in the Early Palaeogene, primarily within the gavialoids. The neosuchian diversification could, in fact, have started during the Maastrichtian and be possibly linked with the Mid-Maastrichtian Event (MME). Dubicka *et al.* (2024) showed that this event has impacted water circulation, sea level, and the marine biota, especially with foraminifera and inoceramids. Although, no clear link between marine vertebrate fauna and the MME has been rigorously demonstrated, Polcyn *et al.* (2014) suggested that the extinction of inoceramids during the MME could have impacted mosasaur diversity with the extinction of the genus *Globidens*. It is, therefore, possible that the MME could have influenced the occupation of different marine ecosystems and consequently favoured the diversification of neosuchians. Moreover, Payne *et al.* (2024) suggested that competition could have stimulated the speciation and the extinction of a lineage. With the generalized extinction from the K–Pg event, recently unoccupied ecological niches would have become available. The colonization of these niches involving competition would have favoured the diversification of marine Neosuchians (Forêt *et al.* 2024). Thus, these competitions would have largely benefited gavialoids, explaining their broad diversification during the Early Palaeogene, while dyrosauroids would have experienced less diversification, in continuity with the Maastrichtian period. Once again, such interpretations should be treated with caution given the limited fossil record for dyrosaurids and the strong taphonomic bias (Fig. 6).

Regarding the evolution rates obtained from our Bayesian analysis, two main remarks can be made. First, the branch of *Atlantosuchus coupatezi* presents a high clock rate, which could be explained by the tree topology. The high clock rate emphasizes the morphological differences of *Atlantosuchus* with the genera *Congosaurus* and *Rhabdognathus*. Notably, *Atlantosuchus* display nine unambiguous synapomorphies. Second, a high clock rate is noticeable at the origin of Dyrosauridae, extending to the Hyposaurinae, corresponding to the interval between 115 and 80 Mya (Fig. 4). This period coincides with the opening of the southern Atlantic Ocean (Granot and Dyment 2015) during which new palaeogeographic and palaeoenvironmental conditions could have favoured the emergence, dispersion, and diversification of Dyrosauridae, thereby explaining the high rate of morphological character changes. This high rate also appears consistent with the predominantly Southern Hemisphere and African origin of the fossils (Fig. 4), as these regions were strongly affected by the palaeogeographic changes associated with the opening of the South Atlantic Ocean. However, it is important to note that this interval is derived from the tip-dating approach used in our Bayesian analysis and might be influenced by the limited availability of fossil material, especially basalmost dyrosaurids, which constrains both temporal and morphological resolution.

Palaeobiogeographical implications

The rich and diverse African dyrosaurid record was synthesized by Amoudji *et al.* (2021) and completed by Jouve and Rodríguez-Jiménez (2023). The discovery of this new Dyrosauridae specimen aligns with the palaeobiogeographic hypotheses proposed by Hastings *et al.* (2015) and Jouve *et al.* (2021). This suggests that MGUAN-PA548 represents a member of migration of longirostrine crocodyliforms in Africa and the South hemisphere during the Maastrichtian. The recent discovery of *Brachiosuchus kababishensis* in the Campanian–Maastrichtian Kababish Formation in Sudan, MUVP 635 in Egypt (Saber *et al.* 2025), in addition to *Sokotosuchus ianwilsoni* and the diverse Hyposaurinae indet. from Sudan (Buffetaut *et al.* 1990, Salih *et al.* 2016) and Mali (Hill *et al.* 2008), suggest an African origin of Dyrosauridae and African migrations during the Campanian–Maastrichtian.

Notably, Bayesian analysis highlights a high rate of character change (clock rate around 2) from the second half of the Cretaceous, coeval with the opening of the Atlantic Ocean during the Upper Cretaceous (Granot and Dyment 2015). The emergence of Dyrosauridae seems to be linked to this event, suggesting that the newly formed ocean facilitated speciation and migration events. With *Brachiosuchus kababishensis*, *Sokotosuchus ianwilsoni*, and the newly described MUVP 536 from the Middle Campanian of Egypt (Saber *et al.* 2025), further supports an African origin for Dyrosauridae, a hypothesis supposed by many authors (e.g. Buffetaut 1976, 1982, Jouve 2005, Barbosa *et al.* 2008, Jouve *et al.* 2008, 2021, Hastings *et al.* 2011, Young *et al.* 2016, Saber *et al.* 2025). However, most of these Cretaceous dyrosaurid fossils originate from inland basins, such as the Iullemmeden Basin, rather than coastal regions directly affected by marine incursions (Fig. 8). Therefore, while the palaeogeographic context may have played a role in broader environmental changes, the link between the South Atlantic opening and dyrosaurid diversification remains hypothetical and should be interpreted with caution.

Thus, MGUAN-PA548 represents one of the Maastrichtian occurrences of Dyrosauridae in the Southern Hemisphere, alongside indeterminate Dyrosauridae from India (Rana 1987, Prasad and Singh 1991, Khosla *et al.* 2009) and possibly from Bolivia (Argollo *et al.* 1987, Gayet *et al.* 1991, 1993). It is also the southernmost record based on current continental distribution. This evidence suggests that Dyrosauridae originated in the Campanian (or earlier) in North Africa and subsequently migrated southwards

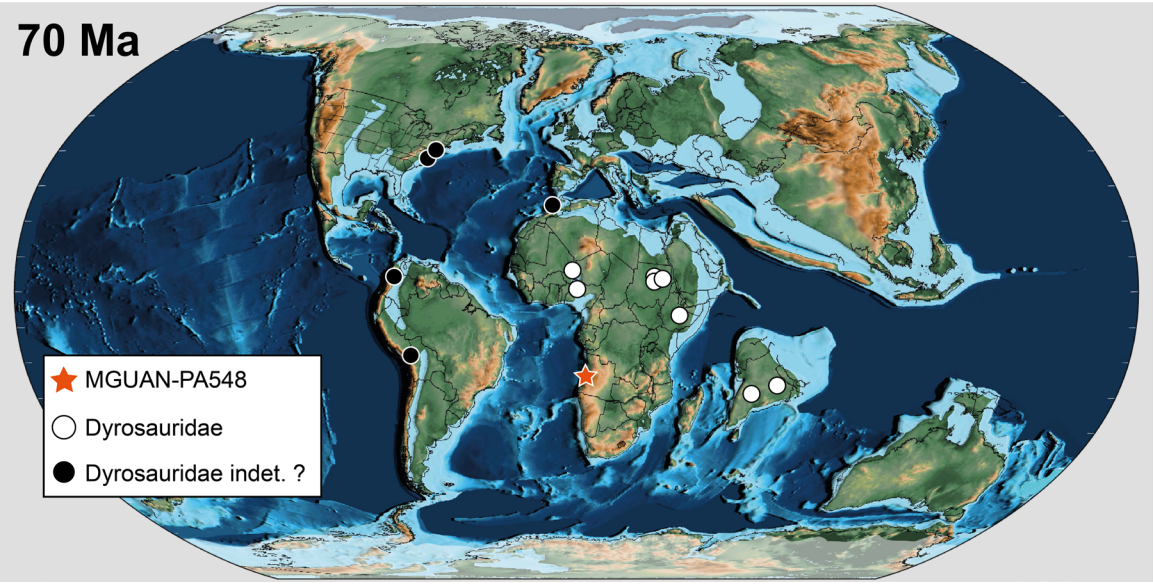

Figure 8. Paleogeographic distribution of dyrosaurid fossils localities from the Late Cretaceous. Map corresponds to the Maastrichtian stage (*c.* 70 Mya), based on Scotese *et al.* (2025) and modified according to Jouve and Rodríguez-Jiménez (2023).

during the Maastrichtian, coinciding with diversification events, including the emergence of Hyposaurinae. These migrations ultimately led to the Palaeocene dispersal and establishment of the Dyrosauridae in South Africa, South America, and North America (e.g. *Hyposaurus natator*). Multiple migration events may have occurred within the clade, with the *Arambourgisuchus*, *Luciasuchus*, and *Dyrosaurus* branch potentially representing an early phylogenetic divergence during the Maastrichtian, likely driven by marine dispersal. This implies that transatlantic exchanges between these continents were more extensive and dynamic than previously proposed by Jouve *et al.* (2021).

The challenges in identifying this specimen, coupled with its fragmentary nature, may be attributed to the fact that MGUANPA-548 is one of the most basal hyposaurine, along with the material from Mali and Sudan (Buffetaut *et al.* 1990, Hill *et al.* 2008, Salih *et al.* 2016). Thus, migrations of Hyposaurinae towards the southern hemisphere could have taken place as early as the Maastrichtian, as alluded to by the Angolan specimen described here. Hyposaurinae, which are thought to have been present along the entire east Atlantic coast since the Maastrichtian, but the dearth of well-preserved, reliably dated fossil material hamper furthers phylogenetic relationships of Palaeogene taxa.

Finally, although beyond the scope of this paper, and in view of the above results and discussions, a complete review of Hyposaurinae is needed. This includes the genera *Rhabdognathus* and *Congosaurus*, as well as *Hyposaurus*, as suggested by Jouve *et al.* (2021), but this is well beyond the scope of this paper. At the risk of complicating the clarity of the phylogenetic relationships of the Dyrosauridae, the association of the new specimen MGUANPA-548 to a new genus seems justified by its distinctive morphological characteristics and by its spatial-temporal location. However, a comprehensive understanding of the dyrosaurid migration in Africa, and the subsequent dispersion throughout the Atlantic, remains unclear and requires further investigation. This includes not only the expanded age calibration of the African occurrences, but a comprehensive analysis of discoveries from the continent, and the exploration for new and more complete fossilized material. Such efforts will contribute to a more comprehensive understanding of the evolutionary history and distribution of Dyrosauridae on both sides of the Atlantic Ocean.

CONCLUSION

We report a new dyrosaurid from the latest Cretaceous of Southern Angola, comprising a posterior portion of the skull, a portion of the left ectopterygoid, and a single tooth. Although the specimen MGUANPA-548 is too fragmentary for precise taxonomic assignment due to the absence of key diagnostic elements such as the mandible, it exhibits a distinctive combination of morphological traits, including a unique autapomorphy, namely the presence of two rounded bosses symmetrically positioned above the foramen magnum in occipital view, that clearly differentiates it from all currently recognized dyrosaurid genera.

Independent phylogenetic analyses allow positioning this specimen as one of the most basal clades within Hyposaurinae. The new remains described here corroborate the palaeobiogeographic hypotheses proposed by Hastings *et al.* (2015) and Jouve *et al.* (2021), suggesting a noticeable diversification of longirostrine crocodyliforms (Dyrosauridae) during the Maastrichtian, despite the pronounced diversification in the Palaeogene, which could reflect some degree of fossil bias. Accordingly, the diversification events of Dyrosauridae during the Palaeogene could eventually reflect previous events during the Maastrichtian, e.g. the Mid-Maastrichtian Event. Considering the recent discoveries of *Brachiosuchus kababishensis*, *Sokotosuchus ianwilsoni*, and MUVP 536, and the relevance of the topic, novel discoveries of Cretaceous Dyrosauridae and additional Maastrichtian Hyposaurinae are expected, which would allow us to elucidate their evolutionary relationships. Ultimately, the various analyses highlight the need of a comprehensive review

of the material associated with Hyposaurinae, as already suggested by Jouve *et al.* (2021).

ACKNOWLEDGEMENTS

For the preparation work, our thanks go out to Filipe Carno and to the Museu da Lourinhã staff, especially to Carla Alexandra Tomas and Micael Martinho for help with the preparation of the specimen. Additional thanks to Francisco Costa for his help with specimen photography, to Douglas Riff who provided photography of the specimen DG-CTG-UFPE 5723, and to Luis Lopes for his help in assembling the 3D model of the specimen. Special thanks to the PalaeoAngola project, namely Anne S. Schulp (Naturalis), Louis Jacobs, and Michael Polcyn (ISEM at SMU). Finally, we would like to deeply thank the two anonymous reviewers for their detailed critiques and suggestions, which greatly improved the quality of the paper.

SUPPLEMENTARY DATA

Supplementary data are available at *Zoological Journal of the Linnean Society* online.

CONFLICT OF INTEREST

None declared.

FUNDING

The research was funded by the Fundação para a Ciência e Tecnología through the project BioGeoSauria (PTDC/CTA-PAL/2217/2021) supporting Arthur Maréchal, Filippo Maria Rotatori, Eduardo Puértolas-Pascual, Cristina Sequero, and Octávio Mateus and by the project GeoBioTec (UIDB/04035/2020: https://doi.org/10.54499/UIDB/04035/2020) supporting Arthur Maréchal, Filippo Maria Rotatori, Cristina Sequero, Ricardo Pereira, and Octávio Mateus. Arthur Maréchal was funded by Fellowship 2022.11517.BD of the Fundação para a Ciência e Tecnología. Filippo Maria Rotatori was funded by Fellowship SFRH/BD/146230/2019 and COVID/BD/153554/2024 of the Fundação para a Ciência e Tecnología. Eduardo Puértolas-Pascual was funded by PID2021-122612OBI00 (Ministerio de Ciencia e Innovación, Government of Spain) and by a postdoctoral contract María Zambrano (Ministerio de Universidades of the Government of Spain through the Next Generation EU funds of the European Union).

REFERENCES

Amoudji YZ, Guinot G, Hautier L *et al.* New data on the Dyrosauridae (Crocodylomorpha) from the Paleocene of Togo. *Annales de Paléontologie* 2021;**107**:102472.

Andrade RCLP, de Sayão JM. Paleohistology and lifestyle inferences of a dyrosaurid (Archosauria: Crocodylomorpha) from Paraíba Basin (Northeastern Brazil). *PLoS One* 2014;**9**:e102189.

Andrade MB, Edmonds R, Benton MJ *et al.* A new Berriasian species of *Goniopholis* (Mesoeucrocodylia, Neosuchia) from England, and a review of the genus. *Zoological Journal of the Linnean Society* 2011; **163**:S66–S108.

Antunes MT, Cappetta H. Sélaciens du Crétacé (Albien-Maastrichtien) d'Angola. *Palaeontographica Abteilung A* 2002;**264**:85–146.

Arambourg C. Note préliminaire sur les vertébrés fossiles des phosphates du Maroc. *Bulletin de la Société géologique de France* 1935;**5**:413–39.

Arambourg C. Les vertébrés fossiles des gisements de phosphates (Maroc-Algérie-Tunisie). *Notes et Mémoires du Service géologique du Maroc* 1952;**92**:1–372.

Arambourg C, Magnier P. Gisements de vertébrés dans le bassin tertiaire de Syrte (Libye). *Comptes rendus hebdomadaires des séances de l'Académie des sciences* 1961;**252**:1181–1183.

Araújo R, Gonçalves AO, Jacobs LL *et al.* New aristonectine elasmosaurid plesiosaur specimens from the Early Maastrichtian of Angola and comments on paedomorphism in plesiosaurs. *Netherlands Journal of Geosciences—Geologie en Mijnbouw* 2015;**94**:93–108.

Argollo J, Buffetaut É, Cappetta H *et al.* Découverte de vertébrés aquatiques présumés paléocènes dans les Andes septentrionales de Bolivie (Rio Suches, synclinorium de Putina). *Geobios* 1987;**20**:123–27.

Barbosa JA, Kellner AWA, Viana, MS, S. New dyrosaurid crocodylomorph and evidences for faunal turnover at the K–P transition in Brazil. *Proceedings of the Royal Society B: Biological Sciences* 2008;**275**: 1385–1391.

Benton MJ, Clark JM. Archosaur phylogeny and the relationships of the Crocodylia. In: MJ Benton (ed.), *The Phylogeny and Classification of the Tetrapods. Vol. 1: Amphibians, Reptiles, Birds*. Oxford: Clarendon Press, 1988, 295–338.

Bergounioux FM. Les crocodiliens fossiles des dépôts phosphatés du Sud-Tunisien. *Comptes rendus hebdomadaires de séances de l'Académie des sciences* 1955;**240**:1917–8.

Bergounioux FM. Les reptiles fossiles des dépôts phosphatés sud tunisiens. *Annales des Mines et de la Géologie* 1956;**15**:1–105.

Brochu CA. Phylogenetic Approaches Toward Crocodylian History. *Annual Review of Earth and Planetary Sciences* 2003;**31**:357–97.

Brochu CA, Bouaré ML, Sissoko F *et al.* A dyrosaurid crocodyliform braincase from Mali. *Journal of Paleontology* 2002;**76**:1060–71.

Bronzati M, Montefeltro FC, Langer MC. Diversification events and the effects of mass extinctions on Crocodyliformes evolutionary history. *Royal Society Open Science* 2015;**2**:140385.

Buffetaut E. Ostéologie et affinités de Trematochampsa taqueti (Crocodylia, Mesosuchia) du Sénonien inférieur d'in Beceten (République du Niger). *Geobios* 1976;**9**:143–98.

Buffetaut E. A dyrosaurid (Crocodylia, Mesosuchia) from the Upper Eocene of Burma. *Neues Jahrbuch für Geologie und Paläontologie, Monatshefte*, 1978a;273–81.

Buffetaut E. Les Dyrosauridae (Crocodylia, Mesosuchia) des phosphates de l'Eocène inférieur de Tunisie : *Dyrosaurus, Rhabdognathus, Phosphatosaurus*. *Géologie Méditerranéenne* 1978b;**5**:237–55.

Buffetaut E. *Sokotosuchus ianwilsoni* and the evolution of the dyrosaurid crocodilians. *The Nigerian Field Monograph* 1979a;**1**:31–41.

Buffetaut E. Présence du crocodilien *Phosphatosaurus* (Mesosuchia, Dyrosauridae) dans le paléocène du Niger et du Mali. *Paläontologische Zeitschrift* 1979b;**53**:323–33.

Buffetaut E. Les crocodiliens paléogènes du Tilemsi (Mali): un aperçu systématique. In: *Palaeovertebrata, Mémoire Jubilaire René Lavocat*. Montpellier: Laboratoire de Paléontologie des Vertébrés de l'Ecole Pratique des Hautes Etudes, 1980, 15–35.

Buffetaut E. Radiation évolutive, paléoécologie et biogéographie des crocodiliens mésosuchiens. *Mémoires de la Société géologique de France* 1982;**142**:1–88.

Buffetaut E, Wouters G. *Atlantosuchus coupatezi* n.g., n.sp., un nouveau Dyrosauride (Crocodylia, Mesosuchia) des phosphates Montiens du Maroc. *Bulletin trimestriel de la Société Géologique de Normandie et des Amis du Muséum du Havre* 1979;**66**:85–90.

Buffetaut E, Bussert R, Brinkmann W. A new nonmarine vertebrate fauna in the Upper Cretaceous of northern Sudan. *Berliner Geowissenschaftliche Abhandlungen* 1990;**120**:183–202.

Callahan WR, Pellegrini R, Schein JP *et al.* A nearly complete specimen of *Hyposaurus rogersii* (Crocodylomorpha, Dyrosauridae) from the Late

Cretaceous–Early Paleogene of New Jersey. *Journal of Vertebrate Paleontology, Program and Abstracts*, 2015;**2015**:101.
Case GR, Cappetta H. A new Selachian fauna from the late Maastrichtian of Texas (Upper Cretaceous/Navarroan; Kemp Formation). *Münchner Geowissenschaftliche Abhandlungen A* 1997;**34**:131–89.
Chiarenza AA, Farnsworth A, Mannion PD *et al.* Asteroid impact, not volcanism, caused the end-Cretaceous dinosaur extinction. *Proceedings of the National Academy of Sciences of the United States of America* 2020;**117**: 17084–93.
Churcher CS, Russell DA. Terrestrial vertebrates from Campanian strata in Wadi El-Gedid (Kharga and Dahkleh Oases), Western Desert of Egypt. *Journal of Vertebrate Paleontology* 1992;**12**:23A.
Cooper MR. The Mid-Cretaceous (Albian/Turonien) Biostratigraphy of Angola. *Annales du Muséum d'Histoire Naturelle de Nice* 1976;**4**: XVI.1–.22.
Cope ED. A contribution to the vertebrate paleontology of Brazil. *Paleontological Bulletin* 1885;**40**:1–20.
Costa B, Fialho P, Balbino A. Occurrence of odontaspidid sharks (Chondrichthyes, Neoselachii) from the Cretaceous of Bentiaba, Angola. *Paleo-Fall Meeting* 2019;**2019**:1.
Denton RK, Dobie JL, Parris DC. The Marine Crocodilian *Hyposaurus* in North America. In: JM Callaway, EL Nicholls (eds), *Ancient Marine Reptiles*. San Diego: Academic Press, 1997, 375–397.
Dollo L. Sur la découverte de téléosauriens tertiaires au Congo. *Bulletin de l'Académie royale de Belgique* 1914;**7**:288–98.
Dubicka Z, Wierny W, Bojanowski MJ *et al.* Multi-proxy record of the mid-Maastrichtian event in the European Chalk Sea: Paleoceanographic implications. *Gondwana Research* 2024;**129**:1–22.
Ehret D, Hastings A. An Eocene occurrence of a dyrosaurid (Crocodylomorpha, Mesoeucrocodylia) from Alabama, USA. *Journal of Vertebrate Paleontology, Program and Abstracts* 2013;**2013**:121.
Erb A, Turner AH. Braincase anatomy of the Paleocene crocodyliform *Rhabdognathus* revealed through high resolution computed tomography. *PeerJ* 2021;**9**:e11253.
Fernandes AE, Mateus O, Andres B *et al.* Pterosaurs from the late cretaceous of Angola. *Diversity* 2022;**14**:741.
Forêt T, Aubier P, Jouve S *et al.* Biotic and abiotic factors and the phylogenetic structure of extinction in the evolution of tethysuchia. *Paleobiology* 2024;**50**:285–307.
Fortier D, Perea D, Schultz C. Redescription and phylogenetic relationships of *Meridiosaurus vallisparadisi*, a pholidosaurid from the Late Jurassic of Uruguay. *Zoological Journal of the Linnean Society* 2011;**163**: S257–S272.
Gayet M, Marshall LG, Sempere T. The Mesozoic and Paleocene vertebrates of Bolivia and their stratigraphic context: a review. *Revista Técnica Yacimientos Petrolíferos Fiscales Bolivianos Santa Cruz, Bolivia* 1991;**12**:393–433.
Gayet M, Sempre T, Cappetta H *et al.* La présence de fossiles marins dans le Crétacé terminal des Andes centrales et ses conséquences paléogéographiques. *Palaeogeography, Palaeoclimatology, Palaeoecology* 1993;**102**: 283–319.
Granot R, Dyment J. The Cretaceous opening of the South Atlantic Ocean. *Earth and Planetary Science Letters* 2015;**414**:156–63.
Guinot G, Condamine FL. Global impact and selectivity of the Cretaceous–Paleogene mass extinction among sharks, skates, and rays. *Science (New York, N.Y.)* 2023;**379**:802–6.
Guinot G, Hautier L, Sambou BS *et al.* The upper cretaceous elasmobranch fauna from Senegal. *Cretaceous Research* 2023;**146**:105480.
Goloboff PA, Farris JS, Nixon KC. TNT, a free program for phylogenetic analysis. *Cladistics* 2008;**24**:774–86.
Halstead LB. *Sokotosuchus ianwilsoni* n.g., n.sp., a new teleosaur crocodile from the upper cretaceous of Nigeria. *Journal of Mining and Geology* 1975;**11**:101–3.
Hastings AK, Bloch JI, Cadena EA *et al.* A new small short-snouted dyrosaurid (Crocodylomorpha, Mesoeucrocodylia) from the Paleocene of northeastern Colombia. *Journal of Vertebrate Paleontology* 2010;**30**: 139–62.
Hastings AK, Bloch JI, Jaramillo CA. A new longirostrine dyrosaurid (Crocodylomorpha, Mesoeucrocodylia) from the Paleocene of northeastern Colombia: biogeographic and behavioural implications for New-World Dyrosauridae. *Palaeontology* 2011;**54**:1095–116.
Hastings AK, Bloch JI, Jaramillo CA. A new blunt-snouted dyrosaurid, Anthracosuchus balrogus gen. et sp. nov. (Crocodylomorpha, Mesoeucrocodylia), from the Palaeocene of Colombia. *Historical Biology* 2015;**27**:998–1020.
Hay OP, 1930. *Second Bibliography and Catalogue of the Fossil Vertebrata of North America*, Vol. **2**. Washington, DC: Carnegie Institution of Washington.
Hill RV, McCartney JA, Roberts E *et al.* Dyrosaurid (Crocodyliformes: Mesoeucrocodylia) fossils from the Upper Cretaceous and Paleogene of Mali: implications for phylogeny and survivorship across the K/T boundary. *American Museum Novitates* 2008;**3631**:1–19.
Jouve S. A new description of the skull of *Dyrosaurus phosphaticus* (Thomas, 1893) (Mesoeucrocodylia: Dyrosauridae) from the Lower Eocene of North Africa. *Canadian Journal of Earth Sciences* 2005;**42**:323–37.
Jouve S. Taxonomic revision of the dyrosaurid assemblage (Crocodyliformes: Mesoeucrocodylia) from the Paleocene of the Iullemmeden Basin, West Africa. *Journal of Paleontology* 2007;**81**:163–75.
Jouve S. Differential diversification through the K–Pg boundary, and post-crisis opportunism in longirostrine crocodyliforms. *Gondwana Research* 2021;**99**:110–30.
Jouve S, Jalil NE. Paleocene resurrection of a crocodylomorph taxon: biotic crises, climatic and sea-level fluctuations. *Gondwana Research* 2020;**85**: 1–18.
Jouve S, Schwarz D. *Congosaurus bequaerti*, a Paleocene dyrosaurid (Crocodyliformes; Mesoeucrocodylia) from Landana (Angola). *Bulletin.de l'Institut Royal des Sciences Naturelles de Belgique, Sciences de la Terre* 2004;**74**:129–46.
Jouve S, Bouya B, Amaghzaz M. A short-snouted dyrosaurid (Crocodyliformes, Mesoeucrocodylia) from the Paleocene of Morocco. *Palaeontology* 2005a;**48**:359–69.
Jouve S, Iarochene M, Bouya B, A, M. A new dyrosaurid crocodyliform from the Paleocene of Morocco and a phylogenetic analysis of Dyrosauridae. *Acta Palaeontologica Polonica* 2005b;**50**:581–94.
Jouve S, Iarochene M, Bouya B *et al.* A new species of *Dyrosaurus* (Crocodylomorpha, Dyrosauridae) from the Early Eocene of Morocco: phylogenetic implications. *Zoological Journal of the Linnean Society* 2006;**148**: 603–56.
Jouve S, Bouya B, Amaghzaz M. A long-snouted dyrosaurid (Crocodyliformes, Mesoeucrocodylia) from the Paleocene of Morocco: Phylogenetic and palaeobiogeographic implications. *Palaeontology* 2008;**51**: 281–94.
Jouve S, de Muizon C, Cespedes-Paz R *et al.* The longirostrine crocodyliforms from Bolivia and their evolution through the Cretaceous–Palaeogene boundary. *Zoological Journal of the Linnean Society* 2021;**192**: 475–509.
Jouve S, Rodríguez-Jiménez JV. The youngest known South American dyrosaurid (Late Paleocene of Colombia), and evolution of Dyrosauridae (Crocodyliformes: Tethysuchia). *Geodiversitas* 2023;**46**: 931–53.
von Koken E. Die Dinosaurier. *Crocodiliden und Sauropterygier des norddeutschen Wealden. Palaeontologische Abhandlungen* 1887;**3**:309–419.
Khosla A, Sertich JJ, Prasad GV *et al.* Dyrosaurid remains from the intertrappean beds of India and the Late Cretaceous distribution of Dyrosauridae. *Journal of Vertebrate Paleontology* 2009;**29**:1321–6.
Kuhn O. *Die Reptilien: System und Stammesgeschichte*. Krailing bei München: Oeben, 1966, 154.
Lamanna MC, Smith JB, Attia YS *et al.* From dinosaurs to dyrosaurids (Crocodyliformes): removal of the post-Cenomanian (Late Cretaceous) record of Ornithischia from Africa. *Journal of Vertebrate Paleontology* 2004;**24**:764–8.
Langston W. Dyrosaurs (Crocodilia, Mesosuchia) from the Paleocene Umm Himar Formation, Kingdom of Saudi Arabia. *Paleocene Vertebrates from Jabal Umm Himar, Kingdom of Saudi Arabia: US Geological Survey Bulletin* 1995;2093-F:F1–F36.
Lewis PO. A likelihood approach to estimating phylogeny from discrete morphological character data. *Systematic Biology* 2001;**50**:913–25.

Martin JE, Amiot R, Lécuyer C *et al.* Sea surface temperature contributes to marine crocodylomorph evolution. *Nature Communications* 2014;**5**: 4658.
Martin JE, Sarr R, Hautier L. A dyrosaurid from the Paleocene of Senegal. *Journal of Paleontology* 2019;**93**:343–58.
Marx MP, Mateus O, Polcyn MJ *et al.* The cranial anatomy and relationships of *Cardiocorax mukulu* (Plesiosauria: Elasmosauridae) from Bentiaba, Angola. *PLoS One* 2021;**16**:e0255773.
Mateus O, Callapez PM, Polcyn MJ, Schulp AS, Gonçalves AO, Jacobs LL. The fossil record of biodiversity in Angola through time: a paleontological perspective. In: *Biodiversity of Angola: Science and Conservation: A Modern Synthesis*. Cham, Switzerland: Springer, 2019, 53–76.
Moody R, TJ,, Buffetaut E. Notes on the systematics and palaeoecology of the crocodiles and turtles of the Metlaoui Phosphates (Eocene) of southern Tunisia. *Tertiary Research* 1981;**3**:125–40.
Morales ME, Goloboff PA. New TNT routines for parallel computing with MPI. *Molecular Phylogenetics and Evolution* 2023;**178**:107643.
Nopcsa BF. The genera of reptiles. *Palaeobiologica* 1928;**1**:163–88.
Norell MA, Storrs GW. Catalogue and review of the type fossil crocodilians in the Yale Peabody Museum. *Postilla* 1989;**N203**:1–28.
O'Leary MA, Bouaré ML, Claeson KM *et al.* Stratigraphy and paleobiology of the Upper Cretaceous–Lower Paleogene sediments from the trans-Saharan seaway in Mali. *Bulletin of the American Museum of Natural History* 2019;**2019**:1–183.
Ortega F, Gasparini ZB, Buscalioni AD *et al.* A new species of *Araripesuchus* (Crocodylomorpha, Mesoeucrocodylia) from the Lower Cretaceous of Patagonia (Argentina). *Journal of Vertebrate Paleontology* 2000;**20**:57–76.
Owen R. Notes on remains of fossil reptiles discovered by Prof. Henry Rodgers of Pennsylvania, U.S., in Greensand Formations of New Jersey. *Quarterly Journal of the Geological Society of London* 1849;**5**:380–3.
Payne ARD, Mannion PD, Lloyd GT *et al.* Decoupling speciation and extinction reveals both abiotic and biotic drivers shaped 250 million years of diversity in crocodile-line archosaurs. *Nature Ecology & Evolution* 2024;**8**:121–32.
Pol, D., and Gasparini, Z.B.. Crocodyliformes. In: ZB Gasparini, L Salgado, RA Coria (eds), *Patagonian Mesozoic Reptiles (Life in the Past)*. Bloomington: Indiana University Press, 2007,116–142.
Polcyn MJ, Jacobs LL, Schulp AS *et al.* The North African mosasaur *Globidens phosphaticus* from the Maastrichtian of Angola. *Historical Biology* 2010;**22**:175–85.
Polcyn MJ, Jacobs LL, Araújo R *et al.* Physical drivers of mosasaur evolution. *Palaeogeography, Palaeoclimatology, Palaeoecology* 2014;**400**:17–27.
Pomel A. Découverte de champsosauriens dans les gisements de phosphorite du suessonien de l'Algérie. *Comptes Rendus de l'Académie des Sciences* 1894;**118**:1309–10.
Prasad GVR, Singh V. Microvertebrates from the intertrappean beds of Rangareddi District, Andhra Pradesh and their biostratigraphic significance. *Bulletin of the Indian Geological Association* 1991;**24**:1–20.
R Core Team. *R: A Language and Environment for Statistical Computing*. Vienna: R Foundation for Statistical Computing, 2023.
Rambaut A. *FigTree*, 2018.
Rambaut A, Drummond AJ, Xie D *et al.* Posterior summarization in Bayesian phylogenetics using Tracer 1.7. *Systematic Biology* 2018;**67**:901–4.
Rana RS. Dyrosaurid crocodile (Mesosuchia) from the infratrappean beds of Vikarabad, Hyderabad District, Andhra Pradesh. *Current Science* 1987;**56**:532–4.
Rasmussen AR, Murphy JC, Ompi M *et al.* Marine reptiles. *PLoS One* 2011;**6**:e27373.
Rio JP, Mannion PD. Phylogenetic analysis of a new morphological dataset elucidates the evolutionary history of Crocodylia and resolves the long-standing gharial problem. *PeerJ* 2021;**9**:e12094.
Ronquist F, Teslenko M, van der Mark P *et al.* MrBayes 3.2: efficient Bayesian phylogenetic inference and model choice across a large model space. *Systematic Biology* 2012;**61**:539–42.
Saber S, Salem BS, Ouda K *et al.* A long-snouted dyrosaurid (Crocodyliformes, Mesoeucrocodylia) from the Campanian Quseir Formation of Egypt. *Cretaceous Research* 2025;**165**:105982.
Salih KAO, Evans DC, Bussert R *et al.* First record of *Hyposaurus* (Dyrosauridae, Crocodyliformes) from the Upper Cretaceous Shendi Formation of Sudan. *Journal of Vertebrate Paleontology* 2016;**36**:e1115408.
Salih KAO, Evans DC, Bussert R *et al. Brachiosuchus kababishensis*, a new long-snouted dyrosaurid (Mesoeucrocodylia) from the Late Cretaceous of North Central Sudan. *Historical Biology* 2022;**34**:821–40.
Schwarz D, Raddatz M, Wings O. *Knoetschkesuchus langenbergensis* gen. nov. sp. nov., a new atoposaurid crocodyliform from the Upper Jurassic Langenberg Quarry (Lower Saxony, northwestern Germany), and its relationships to *Theriosuchus*. *PLoS One* 2017;**12**:e0160617.
Schwarz D, Salisbury SW. A new species of *Theriosuchus* (Atoposauridae, Crocodylomorpha) from the Late Jurassic (Kimmeridgian) of Guimarota, Portugal. *Geobios* 2005;**38**:779–802.
Schwarz-Wings D, Frey E, Martin T. Reconstruction of the bracing system of the trunk and tail in hyposaurine dyrosaurids (Crocodylomorpha; Mesoeucrocodylia). *Journal of Vertebrate Paleontology* 2009;**29**:453–72.
Scotese CR, Vérard C, Burgener L *et al.* The cretaceous world: plate tectonics, palaeogeography and palaeoclimate. *Geological Society, London, Special Publications* 2025;**544**:31–202.
Sertich J, Manthi FK, Sampson F *et al.* Rift valley dinosaurs: a new Late Cretaceous vertebrate fauna from Kenya. *Journal of Vertebrate Paleontology* 2006;**26**:124A.
Simões TR, Greifer N, Barido-Sottani J *et al.* EvoPhylo: an r package for pre- and postprocessing of morphological data from relaxed clock Bayesian phylogenetics. *Methods in Ecology and Evolution* 2023;**14**: 1981–93.
Souza RG, Figueiredo RG, Azevedo SAK *et al.* Systematic revision of *Sarcosuchus hartti* (Crocodyliformes) from the Recôncavo Basin (Early Cretaceous) of Bahia, northeastern Brazil. *Zoological Journal of the Linnean Society* 2019;**188**:552–78.
Stadler T. Sampling-through-time in birth–death trees. *Journal of Theoretical Biology* 2010;**267**:396–404.
de Stefano G. Nuovi rettili degli strati a fosfato della Tunisia. *Bolletino della Società Geologia Italiana* 1903;**22**:51–80.
Strganac C, Salminen J, Jacobs LL *et al.* Carbon isotope stratigraphy, magnetostratigraphy, and 40Ar/39Ar age of the Cretaceous South Atlantic coast, Namibe Basin, Angola. *Journal of African Earth Sciences* 2014;**99**:452–62.
Strganac C, Jacobs LL, Polcyn MJ *et al.* Stable oxygen isotope chemostratigraphy and paleotemperature regime of mosasaurs at Bentiaba, Angola. *Netherlands Journal of Geosciences—Geologie en Mijnbouw* 2015a;**94**:137–43.
Strganac C, Jacobs LL, Polcyn MJ *et al.* Geological setting and paleoecology of the Upper Cretaceous Bench 19 Marine Vertebrate Bonebed at Bentiaba, Angola. *Netherlands Journal of Geosciences—Geologie en Mijnbouw* 2015b;**94**:121–36.
Swinton WE. On fossil reptilia from Sokoto province. *Bulletin of the Geological Survey of Nigeria* 1930;**13**:9–56.
Swinton WE. On *Congosaurus bequaerti* Dollo. *Annale du Musée du Congo Belge* 1950;**13**:9–56.
Tessier F. Contributions à la stratigraphie et à la paléontologie de la partie Ouest du Sénégal (Crétacé et Tertiaire). *Gouvernement Général de l'Afrique Occidentale Française. Bulletin de la Direction des Mines* 1952;**14**:7–569.
Thévenin A. Le *Dyrosaurus* des phosphates de Tunisie. *Annales de Paléontologie* 1911;**7**:95–108.
Troxell EL. *Hyposaurus*, a marine crocodilian. *American Journal of Science* 1925;**s5-9**:489–514.
Walker AD. A revision of the Jurassic reptile *Hallopus victor* (Marsh), with remarks on the classification of crocodiles. *Philosophical Transactions of the Royal Society of London, Series B, Biological Sciences* 1970;**257**: 323–72.
Whetstone KN, Whybrow PJ. A 'cursorial' crocodilian from the Triassic of Lesotho (Basutoland), southern Africa. *Occasional Papers of the Museum of Natural History. The University of Kansas* 1983;**106**:1–37.
Wilberg EW. What's in an outgroup? The impact of outgroup choice on the phylogenetic position of Thalattosuchia (Crocodylomorpha) and the origin of Crocodyliformes. *Systematic Biology* 2015;**64**:621–37.

Wilberg EW, Turner AH, Brochu CA. Evolutionary structure and timing of major habitat shifts in Crocodylomorpha. *Scientific Reports* 2019;**9**:514.

Young MT, Andrade MB. What is *Geosaurus*? Redescription of *G. giganteus* (Thalattosuchia, Metriorhynchidae) from the Upper Jurassic of Bayern, Germany. *Zoological Journal of the Linnean Society* 2009;**157**:551–85.

Young MT, Andrade MB, Cornée J-J *et al.* Re-description of a putative Early Cretaceous 'teleosaurid' from France, with implications for the survival of metriorhynchids and teleosaurids across the Jurassic-Cretaceous Boundary. *Annales de Paléontologie* 2014;**100**:165–74.

Young MT, Hastings AK, Allain R *et al.* Revision of the enigmatic crocodyliform *Elosuchus felixi* de Lapparent de Broin, 2002 from the Lower–Upper Cretaceous boundary of Niger: potential evidence for an early origin of the clade Dyrosauridae. *Zoological Journal of the Linnean Society* 2016;**179**:377–403.